

A novel checkpoint pathway controls actomyosin ring constriction trigger in fission yeast

Tomás Edreira, Rubén Celador, Elvira Manjón, Yolanda Sánchez*

Instituto de Biología Funcional y Genómica, CSIC/Universidad de Salamanca and Departamento de Microbiología y Genética, Universidad de Salamanca, Salamanca, Spain

Abstract In fission yeast, the septation initiation network (SIN) ensures temporal coordination between actomyosin ring (CAR) constriction with membrane ingression and septum synthesis. However, questions remain about CAR regulation under stress conditions. We show that Rgf1p (Rho1p GEF), participates in a delay of cytokinesis under cell wall stress (blankophor, BP). BP did not interfere with CAR assembly or the rate of CAR constriction, but did delay the onset of constriction in the wild type cells but not in the *rgf1Δ* cells. This delay was also abolished in the absence of Pmk1p, the MAPK of the cell integrity pathway (CIP), leading to premature abscission and a multi-septated phenotype. Moreover, cytokinesis delay correlates with maintained SIN signaling and depends on the SIN to be achieved. Thus, we propose that the CIP participates in a checkpoint, capable of triggering a CAR constriction delay through the SIN pathway to ensure that cytokinesis terminates successfully.

Introduction

Cytokinesis in fission yeast, as in most eukaryotes, involves the function of a contractile ring of actin filaments and myosin-II (AR) placed between the poles of the mitotic spindle during cell division. CAR constriction promotes division furrow ingression, so that sister chromatids are segregated to opposing sides of the cleavage plane (Cheffings *et al.*, 2016; D'Avino *et al.*, 2015; Glotzer, 2017; Meitinger and Palani, 2016; Pollard and Wu, 2010; Rincon and Paoletti, 2016; Willet *et al.*, 2015). The failure of this critical step may result in genome instability and contributes to tumorigenesis (Ganem *et al.*, 2007; Nähse *et al.*, 2017; Normand and King, 2010).

The CAR of *S. pombe* is composed of short actin filaments bundled and oriented largely parallel to the PM (Kamasaki *et al.*, 2007), and contains myosin IIs that pull on the actin filaments (Laplante *et al.*, 2015; Mishra *et al.*, 2013). CAR dynamics is tightly regulated in space and time and can be divided into several steps including positioning, assembly, maintenance, constriction, and disassembly. Ring position is determined during interphase by a broad band of cortical cytokinetic precursor nodes localized around the equator (Akamatsu *et al.*, 2014; Moseley *et al.*, 2009). These nodes mature further at mitosis entry when the anillin Mid1p becomes activated by the polo kinase Plo1p (Almonacid *et al.*, 2011; Bähler *et al.*, 1998), which initiates the recruitment of additional cytokinetic factors, including the IQGAP Rng2, Myosin II heavy and light chains (Myo2p, Cdc4p, and Rlc1p), the F-BAR protein Cdc15p and the formin Cdc12p (Laporte *et al.*, 2011; Padmanabhan *et al.*, 2011). Upon mitotic entry, more Mid1p binds to the PM, anchoring ring proteins (and then the ring itself) to this structure (Celton-Morizur *et al.*, 2004; Sohrmann *et al.*, 1996).

Ring assembly takes place between 10 and 15 min after SPB separation driven by interactions between actin filaments assembled by Cdc12p and Myo2p in adjacent nodes (Vavylonis *et al.*,

*For correspondence: ysm@usal.es

Competing interests: The authors declare that no competing interests exist.

Funding: See page 25

Received: 26 May 2020

Accepted: 24 October 2020

Published: 26 October 2020

Reviewing editor: Mohan K Balasubramanian, University of Warwick, United Kingdom

© Copyright Edreira *et al.* This article is distributed under the terms of the [Creative Commons Attribution License](https://creativecommons.org/licenses/by/4.0/), which permits unrestricted use and redistribution provided that the original author and source are credited.

2008; Wu et al., 2006). Once formed, the ring is maintained until the completion of anaphase in an interval known as maturation that lasts ~10 min until the onset of ring constriction. During maturation, the CAR does not change in size or shape, but many proteins are exchanged with others from the cytoplasmic pool (Pelham and Chang, 2002; Roberts-Galbraith et al., 2009). Mid1p disappears, and new F-BAR proteins and partners (Imp2p, Pxl1p, Fic1p) (Roberts-Galbraith et al., 2009), together with unconventional myosin-II (Myp2p) (Laplante et al., 2015) and the glucan synthase Bgs1p (Goss et al., 2014) join the ring.

Ring maintenance, constriction and septum formation depends on the septation initiation network (SIN). This network localizes to the SPB throughout the cell cycle, but also accumulates at the division site immediately prior to cytokinesis and is thought to transmit the signal to the CAR (Goyal et al., 2011; Johnson et al., 2012; Simanis, 2015). The SIN signal begins with the activity of the GTPase Spg1p and involves a regulatory GAP complex, several scaffolds and a linear cascade of three kinases (Cdc7p, Sid1p, and Sid2p), in order of their activation. Substrates of the Sid2p kinase are the phosphatase Clp1p/Flp1p (Mishra et al., 2005), the formin Cdc12p (Bohnert and Gould, 2012), the SIN scaffold Cdc11p (Feoktistova et al., 2012), the kinesin Klp2p (Mana-Capelli et al., 2012), the SAD kinase Cdr2p (Rincon et al., 2017), the anillin Mid1p (Willett et al., 2019) and several others (Grallert et al., 2012; Gupta et al., 2013). Overexpression of Rho GTPase Rho1p, its GEFs Rgf1p and Rgf3p, as well as inactivation of Rho1p GAPs, partially rescues the lethality of *sid2* mutants at a low-restrictive temperature (Alcaide-Gavilán et al., 2014; Jin et al., 2006). Based on these results, it has been proposed that the SIN activates Rho1p, which in turn activates the Bgs enzymes (Jin et al., 2006). However, the SIN target(s) involved in septum assembly remain unknown nowadays.

Both the SIN activity and the CAR are required for septum biosynthesis and the septum in turn contributes to CAR stabilization and constriction (García Cortés et al., 2016; Proctor et al., 2012; Thiyagarajan et al., 2015; Willett et al., 2015; Zhou et al., 2015). As the CAR constricts at a constant rate, the PM ingresses from the cell surface at the medial division site, with the extracellular cell wall just outside the PM, and the contractile ring attached to the membrane on the cytoplasmic side. Thus, septum biosynthesis is coupled to CAR constriction in fission yeast (García Cortés et al., 2016; Roncero and Sánchez, 2010).

Rho GTPases are key regulators of the actin cytoskeleton and their role in cytokinesis has been well established (Glotzer, 2017; Yoshida et al., 2006). In addition, local activation of Rho GTPases at the cleavage furrow promotes contractile ring formation in *Dictyostelium* and metazoans (Wagner and Glotzer, 2016) and activates formins in *S. cerevisiae*, *Dictyostelium*, and metazoans (Kühn and Geyer, 2014). In *S. pombe*, they appear to have none of the previously described functions. Rho1p is involved in regulation of the septum cell wall, but it has not yet been determined whether Rho1p plays a role in the early steps of cytokinesis (García Cortés et al., 2016).

Fission yeast Rho1p is a functional homologue of human RhoA and budding yeast Rho1p (Nakano et al., 1997). Rho1p-GTP binds and activates the protein kinases of the PKC family, Pck1p, and Pck2p (Pérez and Rincón, 2010b), which function upstream of the MAPK module (Mkh1p, Skh1p/Pek1p, and Pmk1p/Spm1p) of the cell integrity signaling pathway (CIP) (García et al., 2009a; Ma et al., 2006; Sánchez-Mir et al., 2014a; Viana et al., 2013). Rho1p is activated by three guanine nucleotide exchange factors (GEFs), Rgf1p, Rgf2p and Rgf3p, that catalyze the exchange from GDP to GTP, rendering the GTPase in an active state (García et al., 2006a; Morrell-Falvey et al., 2005; Mutoh et al., 2005; Tajadura et al., 2004). Rgf1p and Rgf2p localize to the septum area, however, to date there is no evidence of their involvement in cell division (García et al., 2009b; G Cortés et al., 2018; García et al., 2006a; Morrell-Falvey et al., 2005; Mutoh et al., 2005). Rgf3p-GFP forms a ring that follows CAR constriction (Morrell-Falvey et al., 2005; Mutoh et al., 2005; Tajadura et al., 2004) sandwiched by the membrane-bound scaffolds Mid1p, Cdc15p, and Imp2p on the outer side and by F-actin and motor proteins on the inner side (McDonald et al., 2017).

Among the Rho1p-GEFs, Rgf1p is the most prominent. Rgf1p is required for the actin reorganization necessary for cells to change from monopolar to bipolar growth during NETO (New End Take Off) and activates the β -(1, 3) glucan synthase (García et al., 2006a; García et al., 2006b). Rgf1p shuttles in and out of the nucleus in interphase, and is accumulated within the cell nucleus in response to replicative stress (Muñoz et al., 2014). Here, we investigate the role of Rgf1p and Rho1p in cytokinesis and show that stress affecting cell wall integrity prevents the completion of cytokinesis on time. This inhibition depends on a signaling pathway that involves the Rho1p GEF,

Rgf1p, the Rho-GTPase, Rho1p, the ScPkc1p orthologue Pck2p, and the MAP kinase Pmk1p, all components of the cell integrity pathway (CIP). Inactivation of this pathway in stressed cells causes defects in septation (Sengar et al., 1997; Toda et al., 1996; Zaitsevskaya-Carter and Cooper, 1997). Thus, we propose that the CIP signaling delays CAR constriction in response to cell wall perturbations to ensure that cytokinesis reaches completion only after the cell has adjusted to the new conditions.

Results

Rgf1p localizes to the contractile acto-myosin ring (CAR) and interacts with CAR components

As described previously, Rgf1p accumulates at actively growing tips during interphase and re-localizes to a central ring during mitosis (García et al., 2006a; Morrell-Falvey et al., 2005; Mutoh et al., 2005). To precisely determine the temporal regulation of Rgf1p localization in cytokinesis, we investigated Rgf1p localization in a strain co-expressing Rgf1p-GFP^{Envy} (Rgf1p-Envy), Rlc1p-tdTomato (myosin regulatory light chain 1) (Le Goff et al., 2000) and Sad1p-DsRed (a component of the spindle pole body (SPB) tagged with DsRed). In fission yeast, the actomyosin ring is assembled before anaphase, whereas its constriction occurs after completion of anaphase (Wu et al., 2003). The medial Rgf1p-Envy signal detected by time-lapse microscopy appeared during anaphase and before the emergence of the primary septum (PS) stained with calcofluor (blankophor, BP) (Figure 1A, medium frame). During actomyosin ring constriction, Rgf1p-Envy was seen nearby the constricting CAR, as well as with the developing septum (Figure 1A). We analyzed by super-resolution microscopy the localization of Rgf1p and that of Rlc1p and compared them by densitometry of the images (Figure 1B). Rgf1p-Envy seemed to follow the Rlc1p-tdTom ring and localized with the advancing septum edge leaving behind a trail as division proceeded (Figure 1B). This means that the Rgf1-GFP ring was located outside of the contractile ring.

To determine whether Rgf1p medial localization was associated with the actomyosin ring, we examined its localization in a β -tubulin *nda3*-KM311 mutant that stalls mitosis with an assembled CAR at the non-permissive temperature (Hiraoka et al., 1984). Rgf1p-GFP was localized to the division site in these prometaphase-arrested cells (50% of the cell population arrested in prometaphase, $n = 50$; Figure 1C). Consistent with this result, Rgf1p-GFP localization to the division plane was severely compromised in mutants defective in CAR assembly, *cdc15-140* (a mutant in the PHC family protein Cdc15 [Fankhauser et al., 1995]), *cdc3-6* (a mutant in profilin), and in AR maintenance, *cdc11-119* and *sid2-250* (mutants of the SIN components Cdc11p and Sid2p, respectively), at the restrictive temperature (Figure 1D, Figure 1—figure supplement 1). Additionally, we generated double mutants lacking Rgf1p and the essential and non-essential components of the CAR, namely *cdc4-8* and *rlc1 Δ* mutants of myosin II light chains, *cdc15-140* and *imp2 Δ* mutants of PCH family members and *cdc12-112* mutant of the cytokinetic formin. The genetic interaction with myosin mutants was weak (Figure 1—figure supplement 2). Strikingly, we found that the conditions in which *cdc15-140* and *cdc12-112* were able to divide and form colonies at 30°C and 32°C, respectively, the double mutants lacking Rgf1p were inviable at these temperatures (Figure 1—figure supplement 2). Altogether, these experiments establish that Rgf1p starts to accumulate in fully formed contractile rings and before the detection of the septum ingression (Blankophor staining), and that it might collaborate with other cytokinetic proteins in proper cell division.

Cytokinesis is temporally blocked in cell-wall-stressed wild-type cells but not in *rgf1 Δ* cells

Next, we studied CAR constriction in wild type and *rgf1 Δ* cells expressing Imp2p-GFP (CAR marker) and Sid4p-GFP (SPB marker) by time-lapse microscopy (Figure 2A). Time zero corresponds to the time of SPB separation (Wu et al., 2003). Wild type and *rgf1 Δ* early anaphase cells contained normal acto-myosin rings. Moreover, cytokinesis in *rgf1 Δ* measured from the onset of SPB separation until the end of CAR constriction, lasted on average 39.9 ± 3.4 min, a duration that is similar to that of the wild-type cells (mean value 41.5 ± 2.6 min) (Figure 2A and C). To visualize septum formation, cells were treated with blankophor (BP), which is a fluorescent dye that specifically binds to linear β -1,3-glucan at the primary septum (Cortés et al., 2007). Interestingly, the addition of BP onto

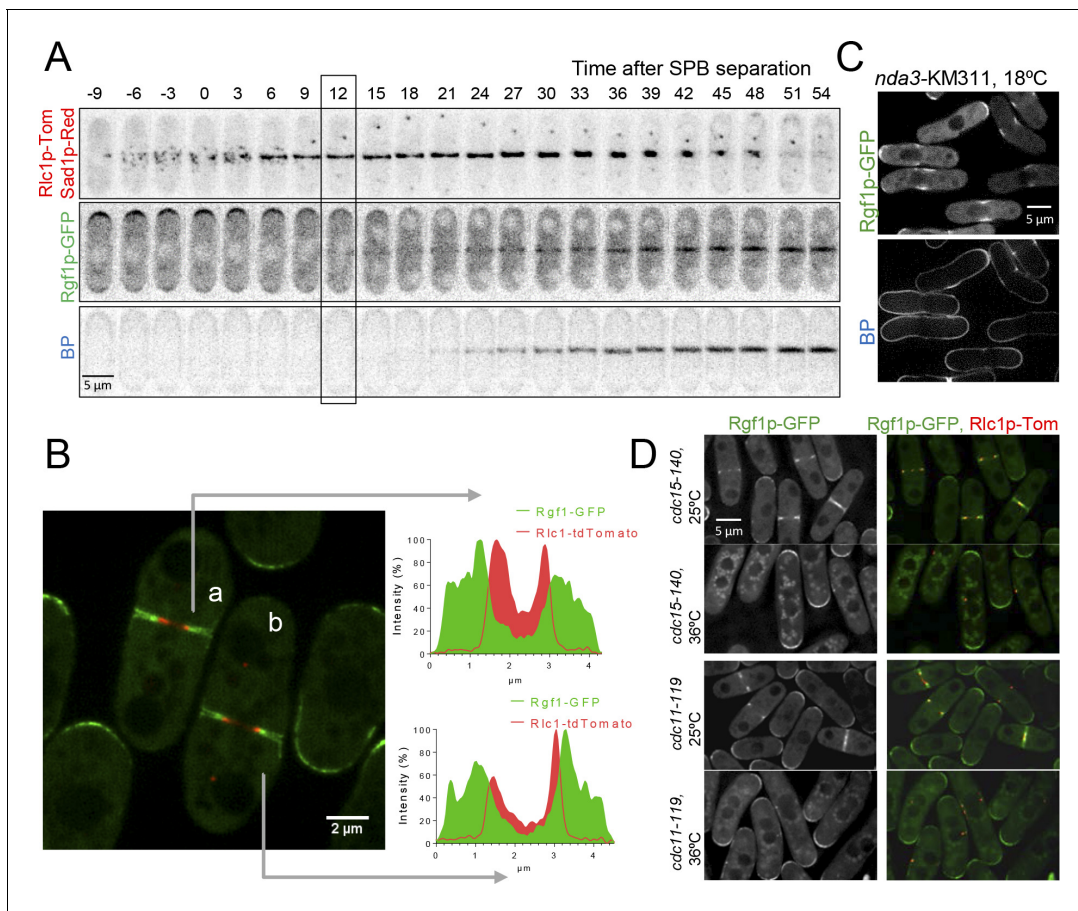


Figure 1. Rgf1p localizes to the contractile acto-myosin ring (AR) during cytokinesis. (A) Time series of fluorescence micrographs (maximum intensity projections of seven sections, inverted grayscale) of a single cell expressing three fluorescent fusion proteins: Sad1p-DsRed to label SPBs; Rlc1p-TdTom to label the ring; and Rgf1p-GFP. Blankophor (BP) 5 μ g/ml was used to mark the septum. (B) Maximum projection of super-resolution images of the same cells as above showing the merged image of the localization of the SPBs (red), Rgf1p (green), and Rlc1p (red). The profile of green and red fluorescence intensity on a line across the division site is shown for cells a, and b, on the right panels. Scale bar 2 μ m. (C) Cell images of *nda3*-KM311 strain expressing Rgf1p-GFP incubated at 18°C for 8 hr before imaging. Cells were stained with BP right before imaging. (D) Maximum projection images of *cdc15-140* and *cdc11-119* cells expressing Rgf1p-GFP and Rlc1p-TdTom. Cells grown at 25°C were transferred 3 hr at 36°C and the images were taken before and after the shift.

The online version of this article includes the following figure supplement(s) for figure 1:

Figure supplement 1. Rgf1p localization in CAR mutants.

Figure supplement 2. Genetic interactions between Rgf1 null mutants and CAR mutants.

wild-type cells caused a delay in the process of cytokinesis (mean value of 59.7 ± 6.7 min, **Video 1**). However, in the *rgf1* Δ cells cytokinesis lasted on average 48.1 ± 6.5 min, a duration which is more similar to the one recorded in the absence of BP treatment (**Figure 2B and C, Video 1**). Then, we performed a titration experiment to determine the time of cytokinesis in wild-type cells treated with different concentrations of BP. As shown in **Figure 2D**, BP caused a dose-effect type delay during our 2 hr movies at 28°C. Thus, for the rest of the experiments we used 5 μ g/ml of BP to induce cytokinesis delay. To further test the effect of BP, we used another combination of markers, Rlc1p-TdTom and Atb2p-GFP (encoding α 2-tubulin that marks microtubules) in *rgf1*⁺ and *rgf1* Δ cells. As above, cytokinesis, measured from spindle formation until Rlc1p-TdTom signal closure at the cell equator, lasted longer in the wild-type cells than in *rgf1* Δ cells treated with BP (n = 15) (**Figure 2—figure supplement 1**). Under these conditions (the presence of BP), CAR contraction was completely blocked (rings did not initiate constriction at any time within the duration of the experiments) in 11 of the 61 wild-type cells examined. Conversely, none of the 83 *rgf1* Δ cells examined blocked cytokinesis

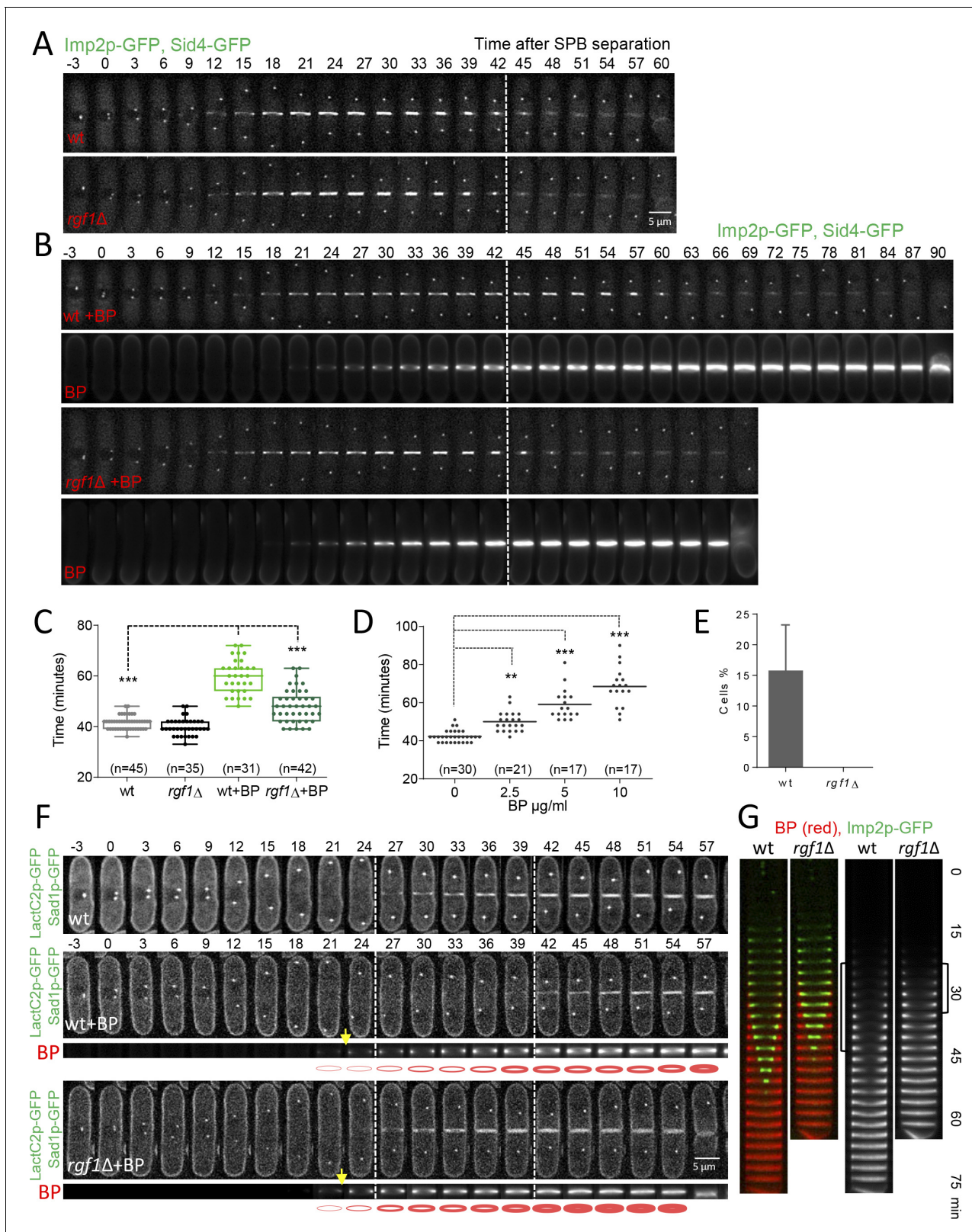


Figure 2. Blankophor (BP) prevents normal cytokinesis. (A, B) Timing of cytokinesis from SPB separation to the end of actomyosin ring contraction. Time-lapse series of wild type and *rgf1Δ* cells expressing Imp2p-GFP (AR marker) and Sid4p-GFP (mitotic marker). Cells grown at 28°C were imaged w/o Blankophor (A) or with Blankophor (5 μg/ml) added just before the time-lapse analysis (B). Images shown are maximum-intensity projections of z stacks. (C) Quantification of (A and B) is shown. Boxes represent the IQR, whiskers are the Tukey's range and the line inside the box is the median. Asterisks indicate statistical significance. Figure 2 continued on next page

Figure 2 continued

indicate the statistical significance of the difference between the two genotypes and the two conditions. Statistical significance was calculated by ANOVA followed by Šidák's multiple comparisons test (n.s. $p > 0.05$; *** $p < 0.0001$). (D) Blankophor (BP) slows down cytokinesis. Cells grown at 28°C were imaged during a time-lapse experiment in the presence of different concentrations of BP. Quantification of the timing of cytokinesis in individual cells of each BP condition is shown. Statistics were performed as in C, comparing each condition with untreated wild type cells (n.s. $p > 0.05$; ** $p < 0.005$; *** $p < 0.0001$). (E) The percentage of wild type and *rgf1Δ* cells treated with 5 μg/ml of BP, where the ring contraction is completely blocked. The data plotted here is the averaged of three independent experiments, with >20 cells for each strain, and the error bars represent the SD of the mean. (F) PM behavior during cytokinesis in BP treated cells. Wild type and *rgf1Δ* expressing Sad1p-GFP (SPB marker) and LactC2-GFP (PM marker) were treated with BP and time-lapse-imaged every 3 min. (t = 0 indicates SPB separation) (lower panels). BP fluorescence images are shown in the lower panels. Wild-type cells w/o BP are shown in the upper panel. (G) Kymographs showing the progression of Imp2-GFP and septum ingression as in (A) in wild type and *rgf1Δ* cells treated with BP.

The online version of this article includes the following source data and figure supplement(s) for figure 2:

Source data 1. Timing of cytokinesis in minutes from SPB separation to the end of actomyosin ring contraction.

Figure supplement 1. Timing of cytokinesis in wild type and *rgf1Δ* cells treated with BP.

Figure supplement 1—source data 1. Timing of cytokinesis in minutes from spindle formation until ring closure.

Figure supplement 2. Septum synthesis is not halted after BP treatment.

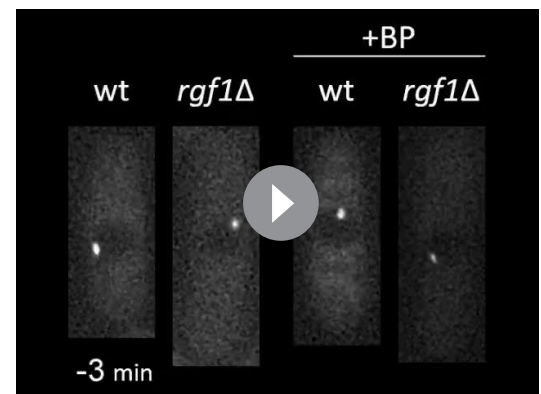
Figure supplement 2—source data 1. BP fluorescence intensity in the septum border over time, with time 0 at SPB separation.

(Figure 2E, Video 2). All together, these data indicate that BP alters the rate of cytokinesis and that this effect is less severe in cells lacking Rgf1p.

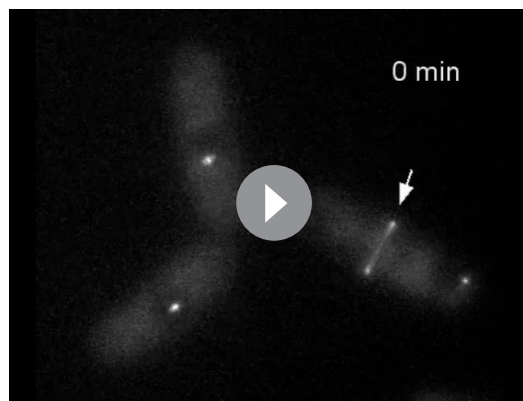
Cell wall stress inhibits PM ingression coupled to CAR constriction

Cytokinesis requires association of the contractile ring with the PM and the cell wall, which in turn pushes the membrane for furrow ingression (Proctor *et al.*, 2012). Defects in these linkages would result in a failure to draw in the PM and a concomitant delay in cytokinesis. In *S. pombe*, proteins like Cdc15p may contribute to the onset of this type of bridging function (Roberts-Galbraith *et al.*, 2010). In addition, Cdc15p promotes the accumulation of glucan synthase (GS) Bgs1p (Arasada and Pollard, 2014), which also contributes to productive ingression. As mentioned above, BP binds to cell wall linear β -1,3-glucan and also interferes with its biosynthesis. Thus, we determined membrane progression and cell wall synthesis during BP treatment. Membrane ingression was followed in cells expressing the LactC2p-GFP fusion protein, which binds to phosphatidylserine at the PM (Yeung *et al.*, 2008). In the absence of BP, the membrane began to ingress ~3 min after spindle breakdown (the moment when the two SPBs with maximum distance began to move toward one another). However, in cells treated with BP, ingression started ~18 min after spindle breakdown, a similar delay as the one detected in CAR constriction (Figure 2F, top panel). Furthermore, ingression was not delayed in *rgf1Δ* cells treated with BP (Figure 2F, lower panel). Thus, BP does not interfere with the linkage between the CAR and the membrane, but temporally inhibits membrane ingression coupled to CAR constriction in wild-type cells.

Interestingly, the BP signal concentrates at the cell equator forming a ring. This fluorescence became noticeable in anaphase, both, in wild type and in *rgf1Δ* cells, indicating that septum synthesis had started regardless of delayed CAR contraction (Figure 2F, yellow arrows and (G Cortés *et al.*, 2018). In the wild-type cells, the initial septum was maintained as a ring that did not progress toward the interior until further on. In *rgf1Δ* cells, the septum progressed more quickly causing the cells to separate earlier than the wild-type cells (Figure 2F). This event can be clearly seen in the kymographs of Figure 2G. From their analysis, it was also inferred that the blockage experienced by wild-type cells, did not halt septum synthesis. This is shown by the fact that BP signal intensity near the cortex



Video 1. Cytokinesis delay under BP treatment. <https://elifesciences.org/articles/59333#video1>



Video 2. Contractile ring blockage under BP treatment.

<https://elifesciences.org/articles/59333#video2>

rgf1⁺ cells expressing mEGFP-Myo2p/Sid4p-RFP, in the presence or absence of BP (5 μg/ml). We analyzed three different stages of the contractile ring progression (**Figure 3A**): CAR assembly (time taken by the mEGFP-Myo2p nodes to coalesce into a ring with homogeneous fluorescence); CAR maturation (the interval between completion of contractile ring assembly and the onset of ring constriction); and CAR constriction (time between CAR diameter shrinkage and the complete closure of the ring). All statistical data are listed in **Table 1**. It was determined that the wild-type cells complete ring assembly within +18 min and +24 min, with a mean completion time of +21.1 ± 2.1 min (mean ± SD) in the absence of BP and 18.6 ± 2.9 in the presence of BP (**Figure 3A and B**). In the case of the *rgf1Δ* mutant, the average time required for the nodes to form a ring was similar to that of the one seen in the wild type either with or without (w/o) BP (**Figure 3B and Table 1**). Thus, Rgf1p does not contribute to contractile ring assembly, which is in accord with its late arrival, to the fully formed ring in wild-type cells (**Figure 1A**). In addition, BP does not alter the ring assembly time.

Next, we measured the amount of time that cells with fully assembled contractile rings spend before constricting. In the wild-type cells ring maturation lasted for approximately 10 min (10 ± 2.8 min, n = 16), while, in the same cells treated with BP the maturation was twice as long, lasting on average 22.1 ± 4.0 min (**Figure 3A and B**). Remarkably, the *rgf1Δ* cells did not exhibit such a prolonged maturation period in the presence of BP (untreated: 8.8 ± 2.5 min, n = 17; BP: 11.4 ± 2.4 min, n = 14) (**Figure 3A and B**). Finally, the time taken for the constricting rings to complete constriction was similar in both strains and conditions (**Figure 3A and B**).

To analyze the onset and the rate of constriction in more detail, first we monitored the time taken for Mid1p-mEGFP to be cleared from the CAR in *rgf1*⁺ and *rgf1Δ* cells treated with BP. Mid1p-mEGFP dissociates from contractile rings during the maturation period (**Sohrmann et al., 1996**). According to the above results, Mid1p-mEGFP dissociated from contractile rings in 16.9 ± 3.1 min in *rgf1*⁺, by contrast the protein dissociated prematurely from the ring in *rgf1Δ* cells (12.0 ± 1.9 min) (**Figure 3—figure supplement 1**). Next, we followed contractile ring constriction in wild type and *rgf1Δ* individual cells marked with Imp2p-GFP/Sad1p-GFP in the presence of BP. In agreement with previous reports (**Ren et al., 2015**), Imp2p localizes to the CAR approximately 15 min after SPB separation, in both, wild type and *rgf1Δ* cells treated with BP (**Figures 2B and 3C**). We measured the ring diameter over time in individual cells (**Figure 3C**), and these plots were used to quantify the onset and rates of ring constriction. The initial rings of Imp2p-GFP of wild type and *rgf1Δ* cells were similar in diameter (wild type: 3.56, *rgf1Δ*: 3.32 μm) and constricted at a similar rate, ~0.15 μm/min. As pointed out above, the mean time for the onset of wild-type ring constriction after SPB separation was +37.9 ± 5.0 min, whereas rings lacking Rgf1p constricted at the cell-cycle time of +25.1 ± 3.6 min, ~13 min earlier (**Figure 3C, Table 1**). Therefore, the presence of BP delayed the onset of constriction beyond the usual time set by the cell-cycle clock. However, the absence of Rgf1p allowed apparently normal ring constriction in BP stressed cells to take place. This behavior suggests that Rgf1p could be part of a mechanism that senses cell wall damage and delays ring constriction while activating repair processes.

increased over time until the onset of constriction (**Figure 2—figure supplement 2**). In sum, fluorescence microscopy showed that ingestion of the ring (Imp2p-GFP), the PM and the stained septum are blocked during anaphase in wild-type cells treated with BP, and that this effect is much less apparent in the *rgf1Δ* cells. These results indicate that wild-type cells respond to cell wall stress with a delay in membrane ingestion and septum progression and that Rgf1p is involved in this novel pathway.

Rgf1p delays the onset of ring constriction in cell-wall-stressed cells

To pinpoint the role of Rgf1p in ring constriction, we followed the behavior of the contractile ring through the time-lapse analysis of *rgf1Δ* and

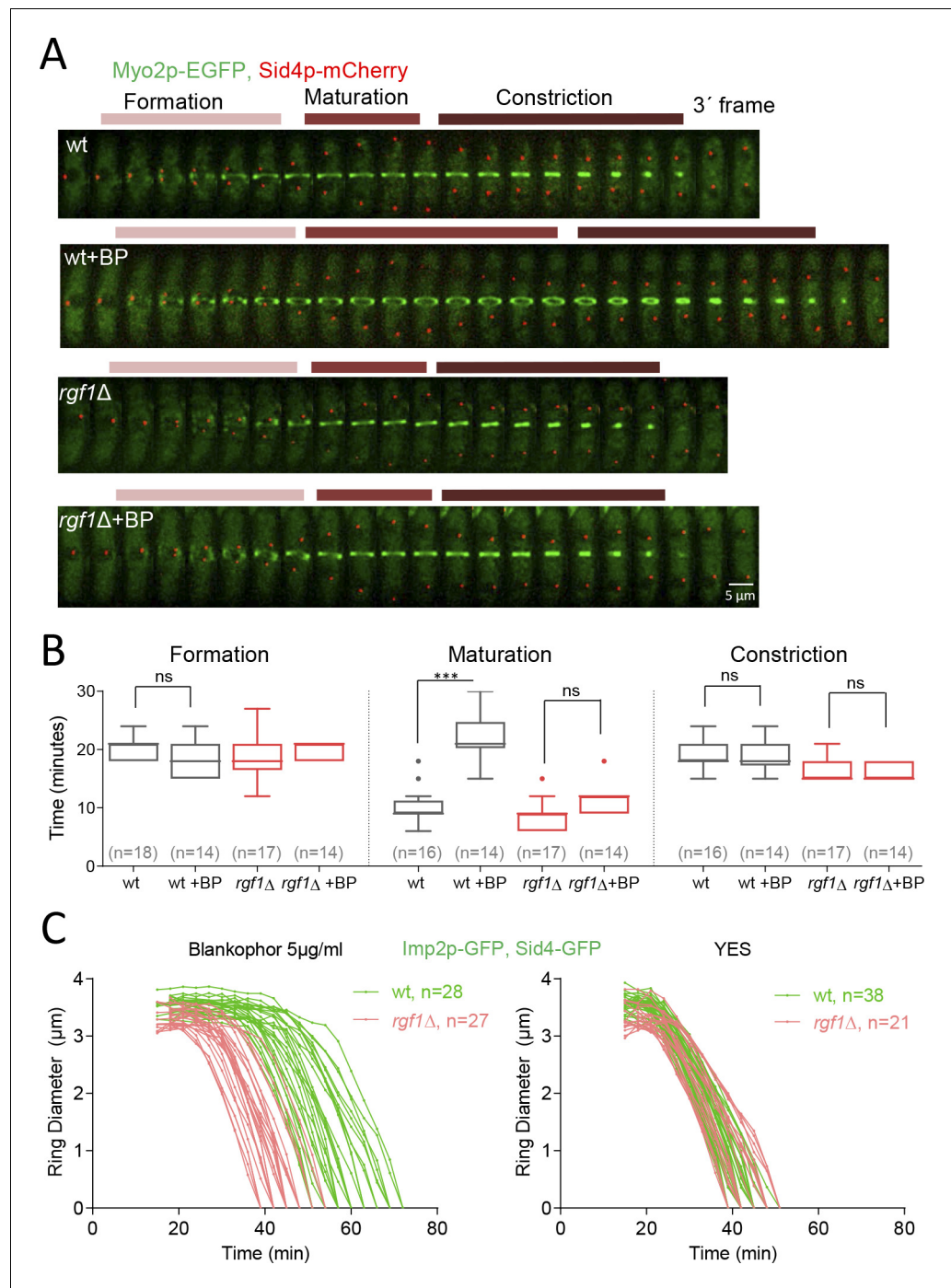


Figure 3. Rgf1p delays the onset of ring constriction in cell wall stressed cells. (A) Time lapse series of wild type and *rgf1Δ* cells expressing Myo2p-EGFP (AR marker) and Sid4p-mCherry (SPB marker). Cells were grown at 28°C and BP (5 μg/ml) was added before imaging, indicated in the panel. The images shown are maximum-intensity projections of z stacks. Scale bars represent 3 mm. (B) The time taken for various steps in cytokinesis (coalescence of nodes into a ring, dwell time before contraction, and contraction). Quantification of (A) was shown. Asterisks indicate the statistical significance of the difference between the two conditions. Statistical significance was calculated by ANOVA followed by Šidák's multiple comparisons test (n.s. $p > 0.05$; *** $p < 0.0001$). (C) Time course of the constriction of the CAR of wild type and *rgf1Δ* cells marked with Imp2p-GFP/Sad1p-GFP, in the presence (5 μg/ml) (right) or its absence (left) of BP, measured as the ring diameter over time, with time 0 min at SPB separation. The graphs show the diameters of each ring.

The online version of this article includes the following source data and figure supplement(s) for figure 3:

Figure 3 continued on next page

Figure 3 continued

Source data 1. Time in minutes taken for various steps in cytokinesis.**Figure supplement 1.** Mid1p-EGFP dissociated prematurely from the ring in *rgf1Δ* cells.**Figure supplement 1—source data 1.** Timing of Mid1-GFP disappearance from the ring.

Rgf1p-dependent inhibition of abscission requires the cell integrity pathway (CIP)

Rgf1p signals upstream from the Pmk1p mitogen-activated protein kinase (MAPK) pathway (García et al., 2009a). This pathway regulates cell wall remodeling, cell separation, and ion homeostasis in injured cells (Loewith et al., 2000; Madrid et al., 2006; Toda et al., 1996; Zaitsevskaya-Carter and Cooper, 1997). Thus, we asked whether the CIP pathway was implicated in sensing BP. To this end, we measured the complete time of CAR constriction (from SPB separation until the end of constriction) in Pmk1p null mutants expressing Imp2p-GFP and Sid4p-GFP under BP stress conditions. While in wild-type cells, cytokinesis lasted a mean value of 59.7 ± 6.7 min in average, in *pmk1Δ* cells the mean value was 44.5 ± 2.8 min, mimicking the pattern of *rgf1Δ* cells (Figure 4A and C, Video 3). Moreover, like the *rgf1Δ*, *pmk1Δ* cells presented a shorter maturation time than that observed in wild-type cells in the presence of BP (*pmk1Δ* BP: 10.9 ± 3.1 min, $n = 22$; wt BP: 22.07 ± 4.0 min, $n = 14$) (Figure 4—figure supplement 1 and Table 1). We also addressed whether this absence of response was due to a lack of kinase activity of Pmk1p under BP stress. *pmk1-KO* cells bearing a kinase-dead mutant version (Pmk1(K52E)GFP) (Sánchez-Mir et al., 2012), phenocopied the absence of cytokinetic response seen in the *pmk1Δ* in the presence of BP (Figure 4—figure supplement 2). These results indicate that Pmk1p signals the delay in the onset of constriction in cell-wall-stressed cells.

Besides the CIP, the stress-response MAP kinase pathway (SRP) affects cell separation under stress conditions. The SRP pathway promotes the transcription of specific gene cohorts and inhibits entry into mitosis in response to damage (Chen et al., 2008a; Petersen and Hagan, 2005; Petersen and Nurse, 2007). Additionally, the SRP has been reported to both promote and attenuate CIP signaling (Loewith et al., 2000; Madrid et al., 2007; Madrid et al., 2006). We checked whether Sty1p/Spc1p (the MAP kinase) was involved in BP sensing and obtained negative results. Cytokinesis in Sty1p null mutant cells lasted a mean value of 57.43 ± 5.1 min, which is similar than that of wild-type cells under BP stress conditions (59.12 ± 8.2) (Figure 4—figure supplement 3).

Next, we analyzed the functional significance of upstream components of the CIP pathway on the cytokinesis delay induced by cell wall stress (Figure 4B). The Rho GTPases, Rho1p and Rho2p, as well as some of its regulators (Rgf1p, Rga4p) and effectors (the protein kinase C PKC orthologues Pck1p and Pck2p) channel different stresses to the MAPK module. However, it is still not well understood which set of components participate in response to each of the initial triggering events. The Rho2p–Pck2p branch is fully responsible for MAPK activation in response to hyper- and hypo-osmotic stresses and both Rho1p and Rho2p target Pck2p for signaling cell wall damage to the CIP. However, the Pmk1p activation observed during cell separation or after treatment with hydrogen peroxide did not involve Rho2p–Pck2p (Barba et al., 2008; Madrid et al., 2015; Sánchez-Mir et al., 2014b). Among the strains assayed, *rgf1Δ* cells (previously shown) and *pck2Δ* were refractory to the

Table 1. Contractile ring parameters.

Genotypes	Formation	Maturation time (min)	Constriction time (min)	Constriction rate (nm/min)
Wild-type	21.1 ± 2.1	9.80 ± 3.2	18.9 ± 2.6	154 ± 21
Wild-type + BP	18.6 ± 2.9	22.1 ± 4.0	18.9 ± 2.7	158 ± 31
<i>rgf1Δ</i>	18.4 ± 3.3	8.08 ± 2.5	16.8 ± 2.1	148 ± 25
<i>rgf1Δ</i> + BP	20.1 ± 1.4	11.4 ± 2.4	16.1 ± 1.5	175 ± 30
<i>pmk1Δ</i>	17.4 ± 1.9	9.79 ± 2.1	16.1 ± 1.7	175 ± 16
<i>pmk1Δ</i> + BP	17.1 ± 2.8	10.9 ± 3.1	16.0 ± 1.9	187 ± 15

Mean \pm SD.

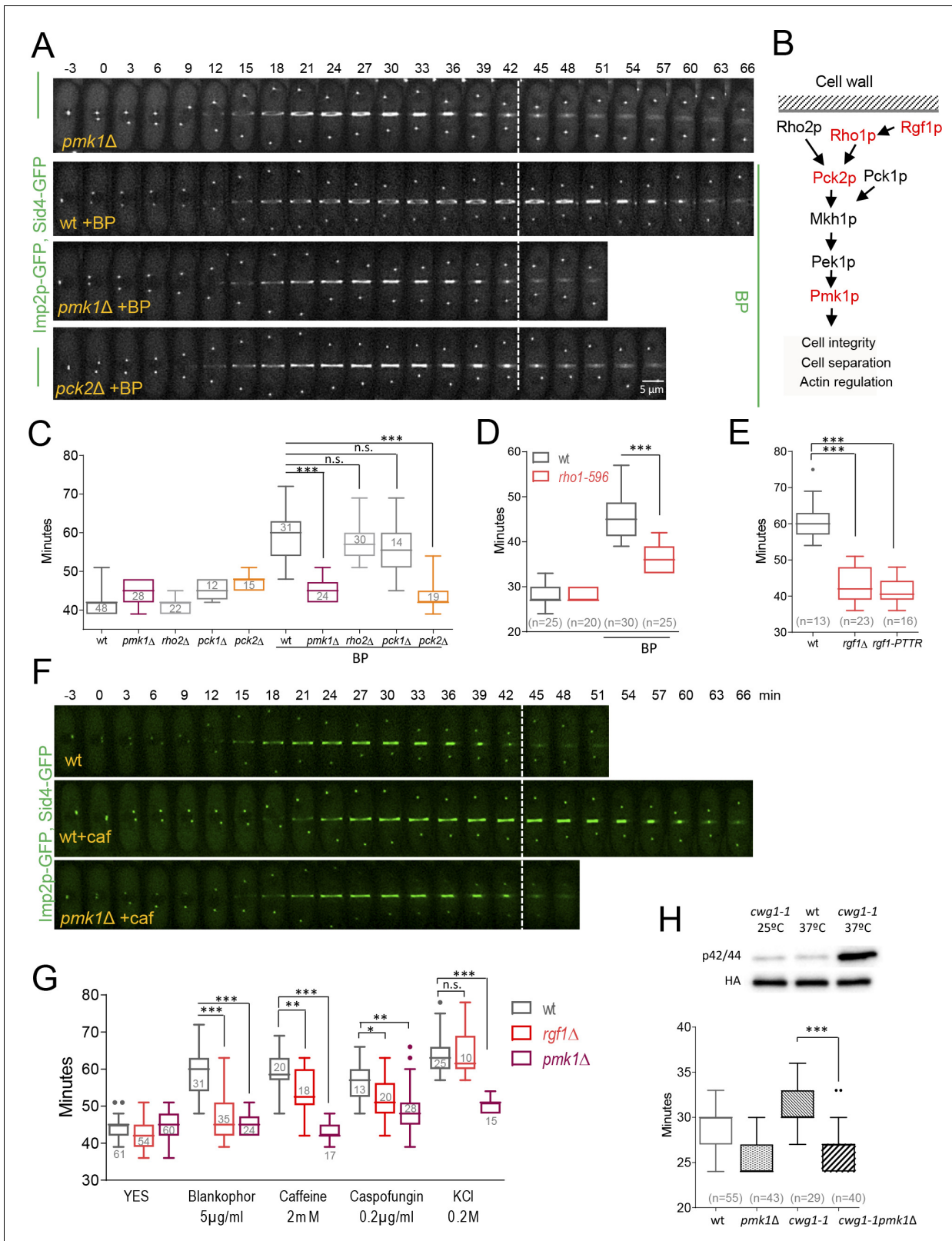


Figure 4. Cell wall stress-induced cytokinesis delay depends on Rho1p and on the cell integrity pathway (CIP). (A) A time-lapse series of wild type, *pmk1Δ* and *pck2Δ* cells expressing Imp2p-GFP (AR marker) and Sid4p-GFP (mitotic marker). Cells were grown at 28°C, and BP (5 μg/ml) was added before imaging when indicated in the panel. The images shown are maximum-intensity projections of z stacks. (B) Scheme of the Pmk1p mitogen-activated protein kinase (MAPK) pathway (CIP). (C) Quantitation of the timing of cytokinesis (from SPB separation to the end of CAR contraction) in wild type, *pmk1Δ*, *pck2Δ*, *rho2Δ*, *rho1-596*, *rgf1Δ* and *rgf1-PTTR* cells. (D) Quantitation of the timing of cytokinesis in wild type and *rho1-596* cells. (E) Quantitation of the timing of cytokinesis in wild type, *rgf1Δ* and *rgf1-PTTR* cells. (F) Time-lapse series of wild type, *pmk1Δ* and *pmk1Δ* cells expressing Imp2p-GFP (AR marker) and Sid4p-GFP (mitotic marker). Cells were grown at 28°C, and caffeine (5 μg/ml) was added before imaging when indicated in the panel. The images shown are maximum-intensity projections of z stacks. (G) Quantitation of the timing of cytokinesis (from SPB separation to the end of CAR contraction) in wild type, *rgf1Δ* and *pmk1Δ* cells treated with YES, Blankophor, Caffeine, Caspofungin or KCl. (H) Western blot and quantitation of the timing of cytokinesis in wild type, *pmk1Δ*, *cwg1-1* and *cwg1-1pmk1Δ* cells. *cwg1-1* cells were grown at 25°C or 37°C. Error bars represent standard deviation. Statistical significance is indicated by asterisks: * p < 0.05, ** p < 0.01, *** p < 0.001, n.s. = not significant.

Figure 4 continued on next page

Figure 4 continued

type, *pmk1Δ*, *rho2Δ*, *pck1Δ* and *pck2Δ* cells expressing Imp2p-GFP and Sid4p-GFP. Cells were grown at 28°C and a time-lapse analysis was carried out in the presence or the absence of BP (5 μg/ml) added before imaging. Asterisks indicate the statistical significance of the difference between the two conditions. Statistical significance was calculated by ANOVA followed by Šidák's multiple comparisons test (n.s. $p > 0.05$; *** $p < 0.0001$). (D) Quantitation of the timing of cytokinesis in wild type and *rho1-596* cells expressing Imp2p-GFP/Sid4p-GFP. Cells were grown at 25°C and shifted to 36°C 1 hr before time-lapse imaging at 36°C. BP (5 μg/ml) was added immediately before imaging. (t = 0 indicates SPB separation). Asterisks indicate the statistical significance of the difference between the two conditions. Statistical significance was calculated by Student's t test (*** $p < 0.0001$). (E) Quantitation of the timing of cytokinesis in wild type, *rgf1Δ*, and *rgf1-PTTR* cells expressing Imp2p-GFP/Sid4p-GFP. Cells were grown at 28°C and a time-lapsed analysis was carried out in the presence of BP (5 μg/ml), added before imaging. Asterisks indicate the statistical significance of the difference between the two conditions. Statistical significance was calculated by ANOVA followed by Fisher's LSD test (*** $p < 0.0001$). (F) Time-lapse series of wild type and *pmk1Δ* cells expressing Imp2p-GFP/Sid4p-GFP. Cells were grown at 28°C and caffeine (2 mM) was added before imaging when indicated. Images shown are maximum-intensity projections of z stacks. (G) Quantitation of the timing of cytokinesis in wild type, *rgf1Δ*, and *pmk1Δ* cells expressing Imp2p-GFP/Sid4p-GFP as in C, in the presence or the absence of BP (5 μg/ml), caffeine (2 mM), caspofungin (0.2 μg/ml), and KCl (0.2M) added before imaging. Statistical significance was calculated by ANOVA followed by Fisher's LSD test (n.s. $p > 0.05$; * $p < 0.05$; ** $p < 0.005$; *** $p < 0.0001$). (H) Upper panel, the wild-type strain and *cwg1-1* mutant, both carrying a HA6H-tagged chromosomal version of *pmk1+*, were grown in YES medium at 25°C and shifted to 37°C for 3 hr. Activated and total Pmk1p were detected with anti-phospho p44/42 and anti-HA antibodies, respectively. Lower panel, quantitation of the timing of cytokinesis in wild type, *pmk1Δ*, *cwg1-1* and *cwg1-1pmk1Δ* cells expressing Imp2p-GFP/Sid4p-GFP. Cells were grown at 25°C and shifted to 36°C 1.5 hr before time-lapse imaging at 36°C. Asterisks indicate the statistical significance of the difference between strains. Statistical significance was calculated by Student's t test (**** $p < 0.0001$).

The online version of this article includes the following source data and figure supplement(s) for figure 4:

Source data 1. Timing of cytokinesis in minutes from SPB separation to the end of actomyosin ring contraction.

Figure supplement 1. Pmk1p delays the onset of ring constriction in cells treated with BP.

Figure supplement 1—source data 1. Time in minutes taken for various steps in cytokinesis.

Figure supplement 2. Timing of cytokinesis in *pmk1-KO* cells treated with BP.

Figure supplement 2—source data 1. Timing of cytokinesis in minutes from SPB separation to the end of actomyosin ring contraction.

Figure supplement 3. Timing of cytokinesis in *sty1Δ* cells treated with BP.

Figure supplement 3—source data 1. Timing of cytokinesis in minutes from SPB separation to the end of actomyosin ring contraction.

Figure supplement 4. Timing of cytokinesis in *rgf1Δ pmk1Δ* cells treated with BP.

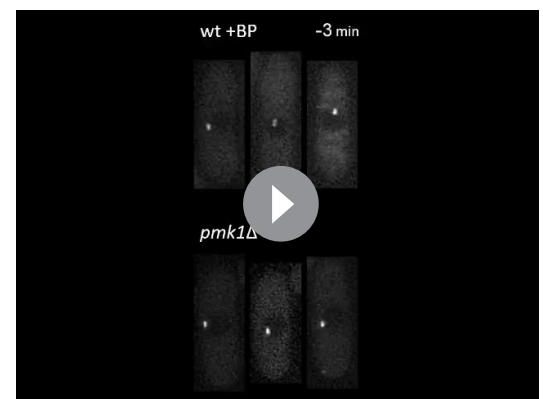
Figure supplement 4—source data 1. Timing of cytokinesis in minutes from SPB separation to the end of actomyosin ring contraction.

Figure supplement 5. Contractile ring constriction in wild-type cells treated with BP, caffeine, caspofungin, and KCl.

Figure supplement 5—source data 1. Ring diameter in μm over time, with time 0 min at SPB separation.

cytokinesis delay induced by BP, while *pck1Δ* and *rho2Δ* mutants behaved like wild-type cells (Figure 4B and C). Moreover, an *rgf1Δ pmk1Δ* double mutant exhibits no synergistic effects in the BP response (Figure 4—figure supplement 4), suggesting that the Rgf1p branch activating Pmk1p (Figure 4B) channels an efficient cytokinesis delay that protects cells from premature abscission under BP stress.

Because Rgf1p acts specifically on the Rho1p GTPase, we tested contractile ring dynamics in a hypomorphic and thermosensitive mutant of Rho1p, *rho1-596* (Viana et al., 2013), in the presence of BP at the restrictive temperature of 36°C. The role of Rho1p in the CIP is controversial and the available literature suggests that the function of Rho1p in the promotion of cell survival during cell wall stress involves both Pmk1p-dependent and -independent pathways (Sánchez-Mir et al., 2014b). Under BP treatment, cytokinesis proceeded faster in the hypoactive mutant (*rho1-596*) than in wild-type cells. However, no differences were found between these strains when left untreated (Figure 4D). Moreover, a deletion mutation in the RhoGEF domain of Rgf1p (*rgf1-PTTR*), which results in significantly reduced GEF activity towards Rho1p (García et al., 2009a), phenocopied the absence of ring constriction delay seen in the Rgf1p



Video 3. *pmk1Δ* cells do not delay cytokinesis under BP treatment.

<https://elifesciences.org/articles/59333#video3>

deletion mutant in the presence of BP (**Figure 4E**). These results indicate that Rho1p is a key player in this process.

Cell-wall-related stresses delay cytokinesis in a CIP-dependent manner

The aforementioned experiments demonstrate that BP blocks cytokinesis temporally in wild-type cells. Thus, we asked whether different treatments disrupting cell wall integrity or affecting the CIP also induce delayed cytokinesis. We used caspofungin (Csp), an inhibitor of the β -1, 3-glucan synthase (**Aguilar-Zapata et al., 2015**), and caffeine (Caf) that activates the Pmk1p cascade signaling in *S. pombe* (**Madrid et al., 2006**) and its orthologue in *S. cerevisiae* (**Kuranda et al., 2006**). Mild treatments with Csp (0.2 μ g/ml) and Caf (2 mM) induced a cytokinesis delay in wild-type cells (**Figure 4F and G, Figure 4—figure supplement 5 and Table 2**). In addition, we found that this delay was almost absent in *pmk1* Δ cells (**Figure 4F and G and Video 4**). In *rgf1* Δ cells, the observed delay was half way between that observed for *pmk1* Δ and wild-type cells (**Figure 4F and G**). The significance of the CIP in reacting to damage inflicted on cell wall structures was further supported by our analysis of the *cwg1-1* mutant cells, which hold a non-lethal thermosensitive mutation in the essential *bgs4*⁺ gene (**Cortés et al., 2005; Muñoz et al., 2013**). We found that Pmk1p becomes phosphorylated in *cwg1-1* cells under restrictive conditions (3 hr at 37°C) (**Figure 4H**). Moreover, this activation of the CIP correlates with a cytokinesis delay in the *cwg1-1* cells, which was also rescued by the elimination of Pmk1p (**Figure 4H**).

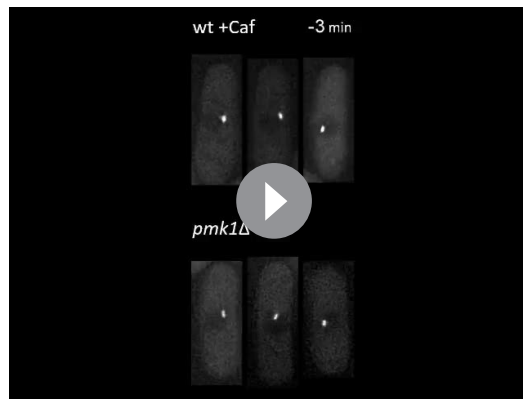
Finally, we addressed whether other adverse conditions that activate the MAPK Pmk1p, such as hyperosmotic stress, might also induce a cytokinesis delay. To this end, KCl (0.6M) was added to the medium to change the osmotic conditions during the time-lapse experiments. In the set-up, the cells shrank, the ring faded and growth temporarily ceased until turgor pressure had adapted (not shown) to the new environment. Under milder conditions, involving less KCl in the medium (0.2M), we did see a transient delay in cytokinesis (>15 min) (**Figure 4G and Figure 4—figure supplement 5**), which was independent on the presence of Rgf1p but dependent on Pmk1p (**Figure 4G**). Although this does not satisfactorily explain the reason for this difference, it could be possible that the other branch of the route, led by Rho2p, accounts for signal transduction under very mild changes in turgor pressure. On the other hand, **Proctor et al., 2012**, have shown that the differential osmotic pressure inside and outside the cell contribute to septum ingression. In these conditions, the phenotype inherent to the mutants (*pmk1* Δ and *rgf1* Δ) and the changes in the turgor pressure imposed by KCl, may explain the different observed behavior. Taken together, the data indicates that in response to mechanical stress, such as a deformed cell wall or stretching of the PM, the CIP temporally blocks CAR constriction.

Mild cell wall stress conditions induce cell separation defects in *pmk1* Δ mutant

MAPK signaling pathways play a key role in eukaryotes to elicit proper adaptive responses to changes in the surrounding or adverse conditions (**Pérez and Cansado, 2010a**). Thus, we investigated the physiological consequences resulting from a compromised Pmk1p function in the presence of mild stress conditions (5 μ g/ml BP, 0,6M KCl, 8 mM Caf); that is, similar conditions that induce an inhibition of CAR constriction in wild-type cells. In agreement with previous data (**Toda et al., 1996; Zaitsevskaya-Carter and Cooper, 1997**), the *pmk1* Δ cells were often shorter and rounder than wild-type cells and sometimes multiseptated cells (2%) were observed (**Figure 5A**). In the absence of stress, we observed a small increase in the septation percentage of *pmk1* Δ cells as compared to the wild-type cells (22% versus 17%) (**Figure 5A and B**). However, under BP treatment, the *pmk1* Δ mutant showed a substantial increase in the number of septated cells

Table 2. Contractile ring parameters in wild-type cells under stresses.

	YES	BP(5 μ g/ml)	Caffeine(2 mM)	Caspofungin (0.2 μ g/ml)	KCl (0.2 M)
Mean Time Constriction Onset (min)	21 \pm 2	38 \pm 5	27 \pm 3	27 \pm 3	27 \pm 3
Mean constriction Rate (nm/min)	154 \pm 21	158 \pm 31	97 \pm 17	114 \pm 13	95 \pm 17



Video 4. *pmk1Δ* cells do not delay cytokinesis under Caf treatment.

<https://elifesciences.org/articles/59333#video4>

(42% with 1 septum plus 26% ≥ 2 septa, $n = 386$ compared to the number of septated cells in the *pmk1⁺* strain) under identical conditions (20% with 1 septum and 0 cells with ≥ 2 septa, $n = 363$) (**Figure 5A and B**). Moreover, a similar increase was detected after treatments with Caf and KCl (**Figure 5A and B**). As expected, multiseptated cells in the *pmk1Δ* mutant walled a nucleus per compartment, indicating that this phenotype was not the result of defective cell cycle control. Thus, the chained-cell phenotype was probably due to the mutant's inability to halt cytokinesis and induce the quality control machinery for septum assembly and/or disassembly.

Effect of myosin and formin inactivation on the delay caused by cell wall stress

Ring constriction is achieved by molecular motors, actin cross-linking proteins and actin branching factors that generate constrictive forces that affect the actin filaments (**Laplante et al., 2015; Mishra et al., 2013; Palani et al., 2017**). To investigate whether this CIP-dependent cytokinesis delay was related to the regulation of the myosin II motor activity, we made use of an unconventional myosin-II *Myp2p* mutant that has a prolonged maturation period and a delay in the onset of ring constriction (**Laplante et al., 2015; Okada et al., 2019; Figure 6—figure supplement 1**). To do so, we treated *myp2Δ* mutant cells with 5 $\mu\text{g/ml}$ of BP (to combine the effects of both methods that postpone ring contraction). Under this condition, the mean constriction time in the cells examined was considerably slower than in the control *myp2Δ* in the absence of BP (*myp2Δ* BP: 60 ± 5.9 min, $n = 16$, *myp2Δ*: 48 ± 5.5 min, $n = 16$). This suggested that the cell wall stress and *Myp2* motor action act independently on the timing of cytokinesis. Similar results were obtained in cells lacking *Rlc1p* (Myosin light chain for *Myo2p* and *Myp2p*). These cells showed a considerable cytokinesis delay (**Sladewski et al., 2009**), which was aggravated in the presence of BP (**Figure 6—figure supplement 1**). These results suggest that these proteins do not bring on the ring constriction delay induced by cell wall stress.

In *S. cerevisiae*, the primary contractile force during budding yeast cytokinesis results from actin depolymerization mediated by cofilin and myosin II motor activity (**Mendes Pinto et al., 2012**). Thus, we explored whether the cytokinesis delay observed after cell wall stress was affected by mutations in the cofilin (*Adf1p*), required for actin severing (**Chen and Pollard, 2011; Nakano and Mabuchi, 2006**), and the formin *Cdc12p* involved in CAR polymerization (**Chang et al., 1997**). The *adf1-1* mutant exhibited a reduced rate in actin depolymerization in vivo (**Nakano and Mabuchi, 2006**). Then, we shifted *adf1-1* mutant at semi-restrictive temperature and monitored the time taken from SPB separation until completion of ring closure. Cytokinesis was slower in the *adf1-1* mutant compared to that of the wild type cells even without cell wall stress induction, indicating that the process was altered under these experimental conditions (**Figure 6—figure supplement 1**). Additionally, *adf1-1* cells showed a significant cytokinesis delay in the presence of BP as compared to their response to non-stress conditions (**Figure 6—figure supplement 1**). Similar experiments were performed using the *cdc12-112* mutant containing a point mutation in the FH2 domain that affects the rate of actin assembly (**Coffman et al., 2013; Figure 6—figure supplement 2**). We found that the *cdc12-112* cells shifted to a semi-restrictive temperature (34°C) and treated with BP act in response to cell wall stress (**Figure 6—figure supplement 2**). These results suggested that actin polymerization/depolymerization defects are not totally necessary for achieving a delay that is imposed by cell wall stress. However, the caveat exists that these temperature-sensitive mutant alleles at the semi-restrictive temperature may not represent a satisfactory loss of function. In fission yeast, *Adf1p* is more important for assembly than for CAR constriction (**Chen and Pollard, 2011**), while cell wall stress seems to affect the maturation steps, which may explain the additive results. Given that *cdc12-112* is affected in the catalytic domain (FHD1) (**Coffman et al., 2013**), the delay

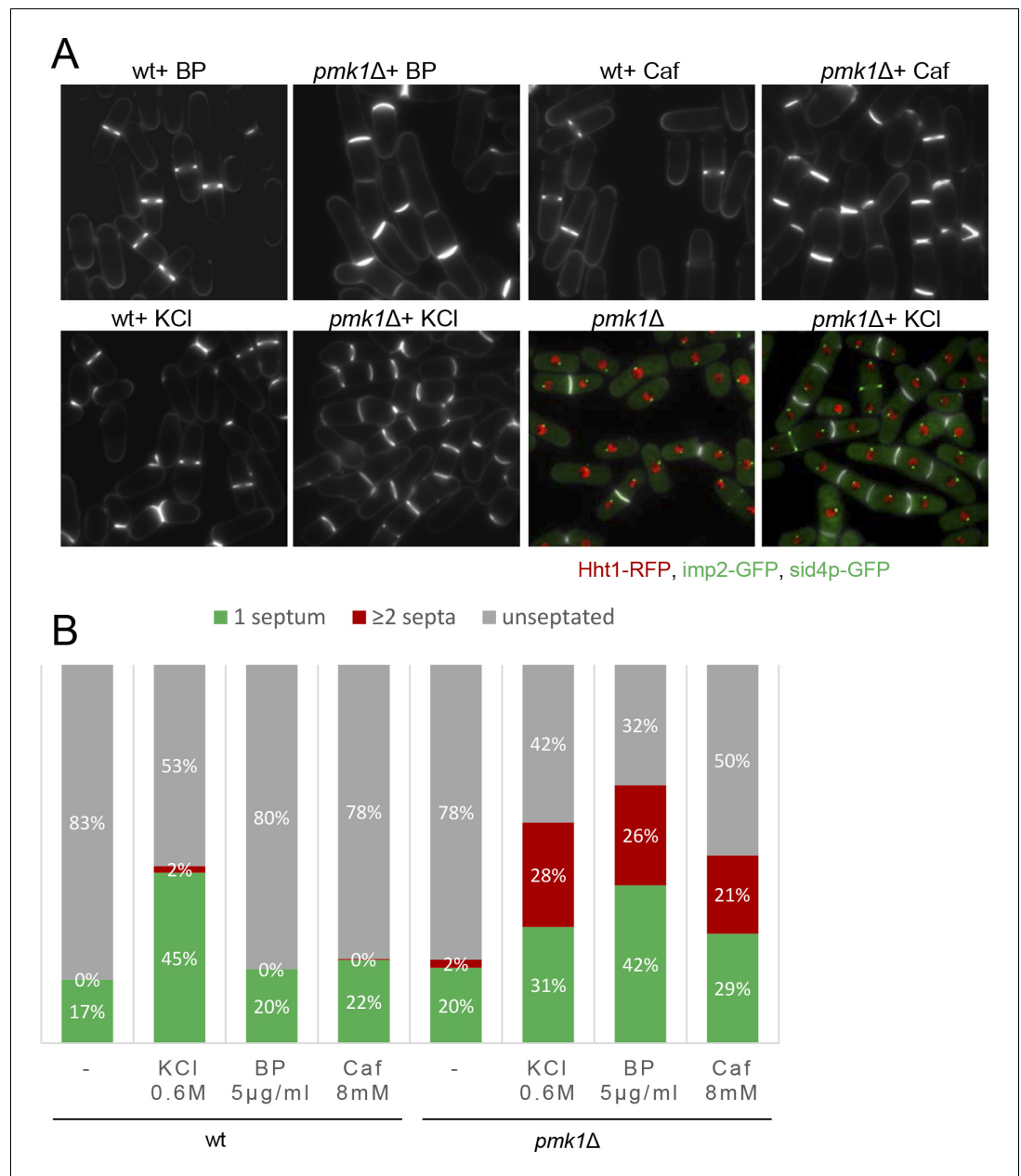


Figure 5. Mild cell wall stress conditions induce cell separation defects in *pmk1Δ* cells. (A) Asynchronous cultures of exponentially growing wild type and *pmk1Δ* cells were treated for 16 hr with KCl (0.6M), BP (5 μg/m) and caffeine (8 mM) at 31°C and then stained with BP to visualize the septum. In the lower panels, the septa, the nucleus, the SPBs and the AR were visualized in wild type and *pmk1Δ* cells expressing Hht1p-RFP (histone H3, h3.1), Imp2-GFP (AR marker) and Sid4p-GFP (SPB marker) and stained with BP right before imaging, before or after KCl treatment. (B) Quantification of A is shown. The number of cells with one septum, ≥2 septa and unseptated cells was quantitated in live cells with or w/o treatment as indicated. Two hundred cells of each strain and condition were analyzed.

seen in the presence of BP could be additive to assembly or maturation defects inherent to the mutant.

Effect of Clp1p inactivation on the delay caused by cell wall stress

In response to the perturbations of the actomyosin ring components, *S. pombe* cells arrest in a 'cytokinesis-competent' state, characterized by continuous repair and maintenance of the actomyosin ring (Mishra *et al.*, 2004) and a G2 block. This checkpoint mechanism requires the function of the phosphatase Clp1p (a Sid2p substrate) (Mishra *et al.*, 2005; Trautmann and McCollum, 2005) and the septation initiation network (SIN) (Le Goff *et al.*, 1999; Liu *et al.*, 2000). In response to cytokinesis defects, Clp1p, normally nucleolar in interphase, is retained in the cytoplasm until completion of cell division in a SIN-dependent manner (Chen *et al.*, 2008b). Consequently, we asked whether BP treatments induce cytoplasmic retention of Clp1p. To this end, we performed a time-lapse analysis of cells expressing Clp1p-GFP, Imp2-GFP and Sid4p-GFP with and w/o cell wall stress (Figure 6A) and quantified the GFP nuclear signal intensity (Figure 6B). Clp1p was released from the nucleolus as cells entered mitosis. In agreement with previous reports (Chen *et al.*, 2008b; Mishra *et al.*, 2005), the protein was not fully re-accumulated in the nucleolus until some minutes after the CAR had finished constriction (~60 min after SPB separation). However, in cells perturbed with low doses of BP Clp1p was released from the nucleolus in a normal way but remained cytoplasmic during the resulting cytokinesis delay (Figure 6A and B). Thus, BP induces cytoplasmic retention of Clp1p. If Clp1p is involved in BP signaling, then, *clp1Δ* mutant cells treated with BP should not display the cytokinetic delay, as *rgf1Δ* and *pmk1Δ* cells do. However, the results shown in Figure 6C indicated just the opposite. In the cells examined, the mean constriction time was considerably slower than in the control *clp1Δ* w/o BP.

Clp1p is known to stabilize the acto-myosin ring in the presence of the actin depolymerizing drug Lat A (Mishra *et al.*, 2005; Trautmann and McCollum, 2005). However, upon BP treatment, the rings appear to be more stable since they do not disassemble when they are blocked, even in the absence of Clp1 (Figure 6C). Thus, in this case, Clp1p would be unnecessary to stabilize the ring. To address the role of BP in the maintenance of the CAR more rigorously, we studied F-actin organization in wild type cells expressing Life Act-GFP endogenously (Huang *et al.*, 2012). These cells were treated with a low dose of LatA (5 μM) in the presence and absence of BP (10 μg/ml) 30 min before starting the time-lapse analysis. In the event that BP could stabilize the ring, we predicted that the F-actin rings would be maintained for a long period of time in cells treated with Lat A in the presence of BP. By contrast, these rings would disappear more quickly in the untreated cells. The proportion of cells with medial F-actin structures was analyzed every 15 min in each condition. Interestingly, the wild-type cells treated with BP were able to maintain, for the duration of the experiment, a higher number of F-actin ring structures (2–3 folds) than the BP-untreated cells (Figure 6D and Video 5). This experiment establishes that upon mild perturbation of the cell wall during cell division the CAR becomes more stable.

In order to check the biochemical status of this stabilised ring, we analyzed the phosphorylation level of Cdc15p. Cdc15p becomes dephosphorylated within mitosis, peaking at anaphase, before it recovers its hyperphosphorylated form right after septation (Clifford *et al.*, 2008; Fankhauser *et al.*, 1995). Cdc15p dephosphorylation, partially dependent on Clp1p, induces its oligomerization, scaffolding activity and stabilizes Cdc15p localization to the division site (Roberts-Galbraith *et al.*, 2010). We generated synchronous cultures by adding HU during 4 hr and released them in fresh medium at 25°C with or w/o BP. Cdc15p becomes dephosphorylated at the same time in the cells that carried BP than in mock cells. However, 120 min after release, we detected a reduced mobility shift of Cdc15p in the cells treated with BP compared to the mock cells (Figure 6E and Figure 6—figure supplement 3). Moreover, Pmk1p absence partially reverted the effect caused by BP in the electrophoretic mobility of Cdc15p, mimicking the kinetics of the untreated cells (Figure 6E and Figure 6—figure supplement 3). These results suggest that ring components are preserved in a stable state during the CAR constriction delay.

Cell wall stress monitors CAR contraction through SIN signaling

Previous studies have shown that SIN mutants assemble actomyosin rings that are not maintained, and disassemble in late anaphase resulting in cytokinesis failure (Simanis, 2015). Thus, we

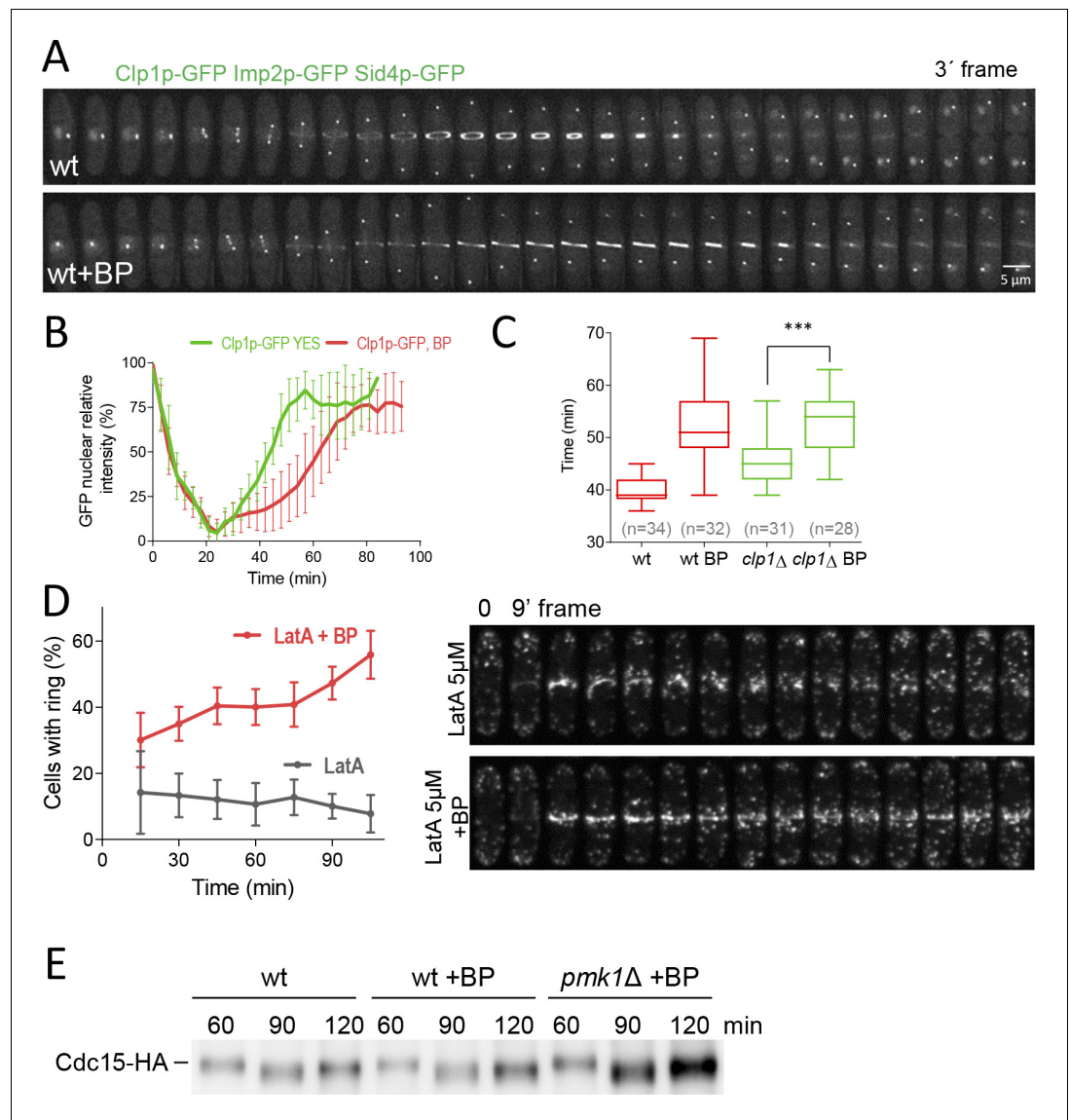


Figure 6. Dynamics of Clp1p-GFP and actin after cell wall stress. (A) Time-lapse images of Clp1p-GFP cells expressing Imp2p-GFP and Sid4p-GFP were collected every 3 min using a DeltaVision microscope. At each time point and position, seven slices were captured with a step size of 0.6 μm. Relative nuclear intensity of GFP over time, starting at SPB separation, is shown in B. (C) Quantitation of the timing of cytokinesis in wild type and *clp1Δ* cells expressing Imp2p-GFP/Sid4p-GFP. Cells were grown at 28°C and a time-lapse was carried out with or w/o BP (5 μg/ml), added before imaging. Statistical significance was calculated by ANOVA followed by Fisher's LSD test (***p*<0.0001) (D) Wild-type cells expressing Life-act-GFP (Huang *et al.*, 2012) grown to log phase at 28°C were treated with a low dose of LatA (5 μM) or with LatA (5 μM) and BP (10 μg/ml) and imaged during a time-lapse (left). The graph shows the percentage of cells with actomyosin rings. Note that in the cells treated with BP the LA-GFP rings are maintained for a prolonged period of time. (E) Protein extracts from Cdc15-HA synchronous cultures, treated or not with BP (1 mg/ml). Early-log phase cells were synchronized by adding HU (12.5 mM) for 4 hr, and then released to fresh medium with or w/o BP. At the indicated times after release, samples were analyzed by western blot using anti-HA antibodies.

The online version of this article includes the following source data and figure supplement(s) for figure 6:

Source data 1. Relative nuclear intensity of GFP over time, starting at SPB separation.

Figure supplement 1. Timing of cytokinesis in *myo2Δ*, *rlc1Δ*, and *adf1-1* mutant cells.

Figure supplement 1—source data 1. Timing of cytokinesis in minutes from SPB separation to the end of actomyosin ring contraction @31°C.

Figure supplement 2. Constriction initiation in *cdc12-112* cells.

Figure 6 continued on next page

Figure 6 continued

Figure supplement 2—source data 1. Time in minutes from SPB separation to the initiation of ring constriction @34°C.

Figure supplement 3. Cdc15p mobility shift in cells treated with BP.

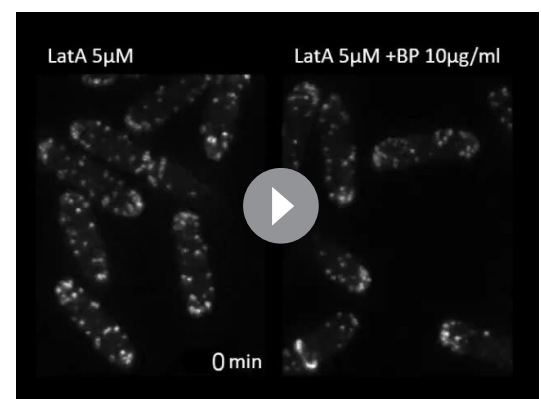
considered the possibility that CAR stability in the presence of mild cell wall stress might be dependent on the SIN pathway. To address this question, *sid2-250* cells expressing Imp2p-GFP and Sid4p-GFP were shifted to a restrictive temperature and treated with BP (10 µg/ml) 30 min prior to being sampled at 2 and 3 hr. Interestingly, the number of rudimentary rings was similar in the presence or absence of BP (Figure 7A), suggesting that the SIN might be involved in CAR stabilization in the presence of cell wall stress.

It is known that localization of Sid2p to the division site, as well as the asymmetric SPB localization of Cdc7p to one SPB, are considered markers of maximal SIN activation and Cdk1p inhibition (Dey and Pollard, 2018; Johnson et al., 2012; Wachowicz et al., 2015). To visualize more closely the state of the SIN under the effect of cell wall perturbation, we imaged wild type (Figure 7B) and *rgf1Δ* cells in combination with these two SIN components (Figure 7—figure supplement 1). In a SIN 'early' state (Wachowicz et al., 2015), Cdc7p localized faintly to both SPBs and similar kinetics were observed in time-lapse experiments involving wild type cells with or w/o BP (Figure 7B). In the 'late' state, the localization of Cdc7p-GFP was asymmetric and lasted until the completion of cell division in both conditions (Figure 7—figure supplement 1). However, the peaked level of Cdc7p dropped after ~30 min in the untreated cells and was maintained at the new SPB for prolonged periods (up to 45 min) in the wild-type cells treated with BP (Figure 7B right and left panels). Sid2p was timely recruited to the ring in the wild type and *rgf1Δ* cells treated with BP, but the protein disappeared earlier from the division site in *rgf1Δ* than in the wild-type cells, just as ring constriction was finishing (Figure 7—figure supplement 1). Similarly, Cdc7p signal at the new SPB lasted longer in wild type than in *rgf1Δ* cells (Figure 7—figure supplement 1). These results strongly suggest: (1) that the delay in constriction induced by cell wall stress is not the consequence of low SIN activity, but instead correlates with a prolonged signal; and (2) that Rgf1p and the CIP may function to extend the duration of SIN signaling upon cell wall perturbations, thereby providing an improved opportunity to constrict the ring properly.

Following on, we asked whether the SIN pathway was required to achieve the cytokinesis delay induced after cell wall stress. At its semi-permissive temperature (32°C), the *sid2-250* strain, partially compromised in Sid2p function is capable of ring formation and constriction. This result, allowed ring dynamics analysis in the presence or absence of cell wall stress. Rings assembled normally in this mutant after 1 hr at 32°C (Figure 7C). However, these cells did not show the delay induced by cell wall stress (Figure 7C). Similar results were obtained using *sid1-239* at the semi-restrictive temperature (Figure 7C), suggesting that SIN signaling is involved in the control of CAR constriction in response to cell wall stress. Based on these studies, we conclude that the SIN is important for initiating the delay in CAR constriction imposed by cell wall stress.

Discussion

The analysis of factors that trigger ring constriction is still one of the least developed aspects of cytokinesis (Pollard, 2017). Here, we show that cell wall damage inflicted during cytokinesis triggers a checkpoint-like response, promoting a delay right before CAR constriction. Sensors relay the signal to the small GTPase Rho1p, triggering phosphorylation events through the cell integrity pathway (CIP). Consequently, inactivation of pathway components by mutations leave the



Video 5. Contractile rings become more stable under BP treatment.

<https://elifesciences.org/articles/59333#video5>

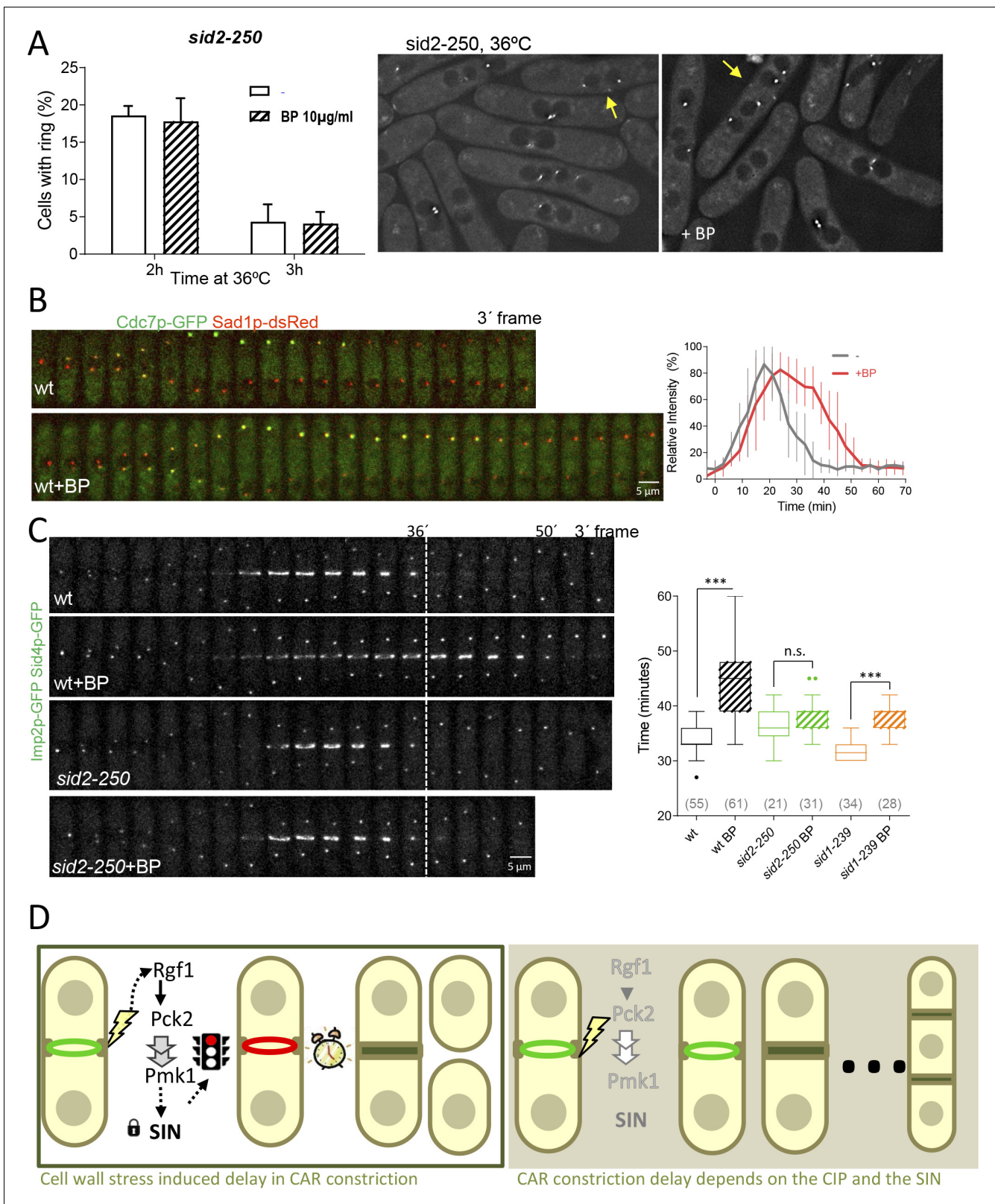


Figure 7. SIN signaling is required for cell wall stress dependent delay. (A) The graph shows quantitative data for *sid2-250* cells expressing Imp2p-GFP/Sid4p-GFP and grown to exponential phase at 25°C. Cultures were shifted to 36°C and imaged after 2 and 3 hr. Thirty minutes before imaging half of the cells were treated with BP (10 µg/ml) (right panels). (B) A time series of the maximum intensity projections of fluorescence micrographs of cells expressing (green) Cdc7p-EGFP and (red) Sad1p-tTomato at 28°C. Cells were imaged w/o BP (top panel) (n = 11) or with BP (5 µg/ml) added (lower panel) (n = 11). (C) Time series of the maximum intensity projections of fluorescence micrographs of cells expressing (green) Imp2p-GFP and (white) Sid4p-GFP at 28°C. Cells were imaged w/o BP (top panel) (n = 11) or with BP (5 µg/ml) added (lower panel) (n = 11). (D) Schematic diagram of the signaling pathway. Cell wall stress induced delay in CAR constriction: Rgf1 activates Pck2, which inhibits Pmk1. Pmk1 inhibits SIN, which is represented by a red traffic light. CAR constriction delay depends on the CIP and the SIN: Rgf1 activates Pck2, which inhibits Pmk1. Pmk1 inhibits SIN, which is represented by a green traffic light.

Figure 7 continued

panel) ($n = 12$) using a spinning-disk confocal microscope. Measurements of Cdc7p-EGFP intensity on the brighter SPB over time in cells with BP (red) or w/o BP (grey) shown in A, with time 0 being SPB separation. (C) Time lapse series of wild type and *sid2-250* cells expressing Imp2p-GFP and Sid4p-GFP. Cells were grown at 25°C and shifted to 32°C 1 hr before time-lapse imaging at 32°C. BP (5 $\mu\text{g/ml}$) was added immediately before imaging. ($t = 0$ indicates SPB separation). Quantitation of the timing of cytokinesis of strains and conditions shown in C. Asterisks indicate the statistical significance of the difference between the two conditions. Statistical significance was calculated by ANOVA followed by Šidák's multiple comparisons test (n.s. $p > 0.05$; *** $p < 0.0001$). (D) Model for CIP-mediated CAR contraction delay caused by cell wall stress in fission yeast cytokinesis. Typically, *rgf1*⁺ and *pmk1*⁺ cells undergo a cytokinesis arrest in the presence of mild cell wall stress. In this context, Pmk1p signal maintains CRs stability in a SIN dependent manner. However, when the signal is blocked in deletion mutants of the CIP components or when the SIN kinase Sid2p is not fully active, the ring is prematurely closed. Persistent cell wall stress leads to the formation of multiseptated cells. Thus, the CIP-mediated signal is transmitted to the SIN that stabilizes AR before constriction and enable proper CAR performance.

The online version of this article includes the following source data and figure supplement(s) for figure 7:

Source data 1. Percentage of cells with actomyosin rings over time, shifted to 36°C at time 0h.

Figure supplement 1. Cell wall stress delays Sid2p silencing in wild-type cells but not in *rgf1* Δ cells.

Figure supplement 1—source data 1. Time in minutes of the arrival and release of Sid2-GFP at the septum.

damage signal unchecked during cytokinesis, which results in premature CAR constriction and leads to the failure of cell cleavage (**Figure 7D**).

In this work, we addressed the question of whether Rgf1p and Rho1p play a role in cytokinesis in addition to their function in septum synthesis (**Pérez et al., 2016**). We confirmed and extended previous observations showing that Rgf1p localizes to the proximity of the assembled ring (**García et al., 2006a; Mutoh et al., 2005**); the protein follows the advancing septum edge leaving behind a trail as division proceeds (**Figure 1**). This localization differs from that of Rgf3p, which forms a ring that disappears at the end of CAR constriction (**Morrell-Falvey et al., 2005; Mutoh et al., 2005**), suggesting a role for Rgf1p in the furrow ingression step. Rgf1p localizes to the assembled ring before the septum is perceived. Interestingly, we found that Rgf1p controls the onset of ring constriction under cell wall stress (Blankophor 5 $\mu\text{g/ml}$), but does not affect CAR dynamics in unperturbed growth conditions. This is probably the reason why Rgf1p function in cytokinesis has been ignored for such a long time. Moreover, the requirement of Rgf1p to delay CAR constriction is due to the activation of Rho1p, as both the *rgf1-PTTR* and *rho1-596* mutants exhibited a lack of ability to delay cytokinesis similar to that of the *rgf1* Δ mutant.

Our work has also built upon what is already known about the contribution of cell wall synthesis to cytokinesis (**Proctor et al., 2012; Zhou et al., 2015**). A recent idea in the field of cytokinesis is that, for walled eukaryotes such as *S. pombe*, the dominant factor determining the rate of ring constriction is not the amount of tension that can be generated in the contractile ring, but rather the rate of synthesis of new cell wall material used to generate the invaginating furrow (**Cheffings et al., 2016; Proctor et al., 2012**). We have shown that treatments that disorganize the cell wall (BP) and delay septum progression also delay CAR constriction (**Figure 2**). This impact is considered significant, as 15% of the cells with assembled rings never go on to complete ring closure; the rest (~85%) show a delay of 12–15 min as compared to the untreated cells. Moreover, cell wall stress influences the onset of CAR constriction, but does not interfere with CAR assembly or the rate of CAR constriction. It is possible that in the temporary absence of a cell wall headway the CAR provides insufficient force to be closed. If BP reduces the force generated by the septum, then the cells could experience an imbalance in force production between the CAR and the septum and the CAR might need to provide additional force (**Proctor et al., 2012**). Alternatively, a regulatory pathway may couple constriction of the CAR and septum formation such that a defect in septum formation could prevent the constriction of the CAR. Some of these possibilities are not mutually exclusive. We have shown that cell wall stress (inflicted by BP) generates a delay of approximately 15 min in CAR constriction, and this has a direct impact on cell separation. Moreover, mutants in Rgf1p, Rho1p, Pck2p, upstream regulators, and Pmk1p, the MAP kinase of the cell integrity pathway, do not exhibit a delay in cytokinesis followed by mild cell wall stress. Other sorts of cell wall damage, such as that caused by a point mutant in the main β -GS, also lead to a delay in cytokinesis that is sensed by the CIP. In addition, mild treatments with antifungal agents like caspofungin and caffeine also behaved similarly.

Time is important. Although, it is known for a long time that the MAP kinase Pmk1p becomes activated 'within minutes' by cell wall stress (**Barba et al., 2008; Madrid et al., 2007**), it is still

unclear how the CIP integrates this stress input with successful cell separation (Bähler, 2005). A quick response is required when the cell's genome has already split and the cell becomes ready to separate its cytoplasm. Cell wall sensors/transducers detect the perturbation in the septum as it starts to form and activate Pmk1p to block cytokinesis progression under the situation of a deficient septum. The pathway can be equally impacted by modulating the phosphatase Pmp1p, which removes the activating phosphorylation on Pmk1p (Sugiura et al., 1998). In the case that the checkpoint is overridden, some septa could be poorly built up. In that sense it is known that conditions of nutrient limitation, hypertonic stress or caffeine, prompt *pmk1Δ* cells to grow as short-branched filaments in which the cell walls and septa are thickened (Zaitsevskaya-Carter and Cooper, 1997). At the same time, Pmk1p might induce the expression of genes that function to replace the damaged wall and restart cytokinesis even under stress conditions (Chen et al., 2003; Takada et al., 2007).

We considered how Pmk1p is able to accomplish CAR regulation after cell wall stress. The coordination mechanism may involve proteins that are physical components of the ring or regulatory proteins that may link the pathways together (Cheffings et al., 2016; Pollard, 2017). In this sense, we have shown that defects in formin and myosin II, that are force-generating components of the CAR, show a delay in CAR maturation (Laplante et al., 2015; Lord et al., 2005; Stachowiak et al., 2014), which was additive to the delay observed during cell wall stress. However, a mutation in the SIN kinase Sid2p was refractory to the delay caused by cell wall stress, indicating that the CIP may act by promoting the maintenance of SIN activity. There is a much evidence that reinforces this premise. First, cell wall stress correlates with a prolonged SIN signal, where Cdc7p remains on the new SPB for more time and the cytoplasmic retention time for Clp1p is longer (Figures 6A and 7B). This does not occur in the *rgf1Δ* and *pmk1Δ* (not shown) mutants where the SIN signal is deactivated earlier (Figure 7—figure supplement 1); these mutants behave like wild-type cells in the absence of cell wall damage. Second, cell wall damage makes contractile rings more stable, where they become less vulnerable to mild perturbations of the actin cytoskeleton. Given that Sid2p is required for CAR maintenance when the cytokinesis checkpoint is active (Alcaide-Gavilán et al., 2014), it is very likely that the prolonged SIN activity serves to maintain the CAR in a competent state to achieve constriction safely. Third, SIN mutants grown at high temperature block the cell wall stress signal (Figure 7A). In these conditions, the rings are not maintained owing to a deficient SIN that is incapable of stabilizing them.

Cytokinetic furrow ingression requires both the actomyosin ring constriction and septum formation. Since one process cannot progress without the other, at least initially, cytokinesis can potentially be arrested through the blockage of either of these two components. There are two reasons that favor the proposal of a blocking model that operates through a halt in the onset of ring constriction. First, septum formation, measured as the increase of BP intake, is not stopped but increases linearly over time even without any trace of ring constriction (Figure 2—figure supplement 2); and second, the CAR becomes stabilized in a SIN-dependent manner after cell wall stress. In this study, we also address how this system is able to block cytokinesis when the ring is already formed, especially considering the onset of ring constriction is one of the least understood aspects of cytokinesis. Although ring constriction usually coincides with full SIN activation, we have shown a situation where the SIN is kept transiently active and the onset of constriction correlates with SIN inactivation. Similar to the cytokinesis checkpoint, Sid2p may well be blocking the onset of ring constriction by its stabilization under cell wall stress, even with a competent GS.

In animal cells, RhoA and RhoGEF Ect2p are key players in cytokinesis. Active Rho A around the equator regulates formins that polymerize actin filaments and kinases that activate myosin-II (Wagner and Glotzer, 2016). In addition, RhoA has a role as a negative regulator of the hippo pathway (the SIN counterpart in mammals) (Plouffe et al., 2016). When deleted RHOA, LATS1/2 (Sid2p counterpart in mammals), and YAP/TAZ (the transcription factor downstream) remained highly phosphorylated; the latest is sequestered in the cytoplasm, and is maintained transcriptionally inactive, even in the presence of serum (Plouffe et al., 2016). According to that, our work in *S. pombe* indicates that Rho1p controls the SIN to achieve ring constriction properly under cell wall stress. Understanding the relationship between Rho1p and the SIN pathway in yeasts would be helpful to grasp how RhoA and the Hippo pathway interact in mammals.

Materials and methods

Key resources table

Reagent type (species) or resource	Designation	Source or reference	Identifiers	Additional information
Antibody	Anti-phospho-p42/44 (Rabbit polyclonal)	Cell Signaling	Cat#: 9101, RRID:AB_331646	WB (1:2500)
Antibody	Anti-HA (Mouse monoclonal)	Roche	Cat# 11666606001, RRID:AB_514506	WB (1:5000)
Antibody	HRP anti-mouse (Goat polyclonal)	Bio-Rad	Cat#: 170-6516, RRID:AB_11125547	WB (1:10000)
Antibody	HRP anti-rabbit (Goat polyclonal)	Bio-Rad	Cat#: 170-5046, RRID:AB_11125757	WB (1:15000)
Chemical compound, drug	Blankophor	Bayer	Blankophor BA 267%	
Chemical compound, drug	KCl	Merck	Cat#: 104936	
Chemical compound, drug	Caffeine	Sigma-Aldrich	Cat#: W222402	
Chemical compound, drug	Caspofungin	Sigma-Aldrich	Cat#: SML0425	
Chemical compound, drug	Latrunculin A	Sigma-Aldrich	Cat#: L5163	
Chemical compound, drug	Hydroxyurea	Sigma-Aldrich	Cat#: H8627	
Chemical compound, drug	Soybean lectin	Sigma Aldrich	Cat#: L2650	
Commercial assay, kit	Ni-NTA	Novagen	Cat#: 70666	
Software, algorithm	GraphPad Prism	GraphPad Prism (https://graphpad.com)	RRID:SCR_015807	
Software, algorithm	ImageJ	ImageJ (http://imagej.nih.gov/ij/)	RRID:SCR_003070	
Other	μ-Slide eight well	Ibidi	Cat#: 80826	

General yeast growth conditions and genetic methods

Standard *S. pombe* genetic procedures and media were used (Forsburg and Rhind, 2006; Moreno et al., 1991). The relevant genotypes and the source of the strains used are listed in Table 3. Unless otherwise stated, the experiments were performed with cells growing exponentially in liquid-rich medium, yeast extract with supplements (YES; 0.5% yeast extract, 3% glucose, 225 mg/l adenine sulphate, histidine, leucine, uracil and lysine, 2% agar) and incubated at 28°C. Geneticin, hygromycin and nourseothricin were used at 120 μg/ml, 400 μg/ml, and 50 μg/ml, respectively. Latrunculin A (stock at 5 mM in DMSO) was used at 5 μM. To Tag Rgf1p with the GFP^{Envy} protein we made use of the integrative plasmid pGR49 (pJK148-*rgf1*⁺-GFP) carrying the GFP^{Envy} in frame in a NotI site just before the TAA stop codon (García et al., 2006a). The GFP^{Envy} was PCR-amplified from plasmid pFA6A-link-envy-SpHis5 (Slubowski et al., 2015) with NotI sites at the ends and sub-cloned into pGR41 instead of the GFP. This plasmid was cut with Eco47III and integrated into the *leu1* locus of an *rgf1*Δ strain. Genetic crosses and selection of the characters of interest by random spore analysis were used to combine different traits (Forsburg and Rhind, 2006). All the deletions strains generated in this work were checked by PCR, drop assays with caspofungin (0,5–1 μg/ml) and the appropriate selection markers.

Microscopy and image analysis

Fluorescence images were acquired on an Olympus IX71 inverted microscope (Olympus) equipped with a PlanApo 100x/1.40 IX70 oil immersion objective, a personal DeltaVision system (GE Healthcare) and a CoolSnap HQ2 camera (Photometrics), all controlled by SoftWoRx Resolve 3D (Applied Precision). Early logarithmic phase cell cultures grown at 25°C were shifted to 36°C for 3 hr. Approximately 100 μl of cells were collected by a short spin, dissolved in 5 μl of water and Calcofluor white (Blankophor BA 267%, Bayer) was added at a final concentration of 50 μg/ml. Then, 10 slices at 0.2 μm were taken, corrected by 3D Deconvolution (conservative ratio, 10 iterations and medium noise filtering) with softWoRx software (GE Healthcare), and processed with Fiji distribution of Image

Table 3. *S. pombe* strains used in this work.

Strains	Genotypes
YS5261	h ⁻ <i>rgf1::kanMX6, leu1-32::rgf1-EnvyGFP, sid4-mcherry:hph, rlc1-tdTomato:nat, ura4D18</i>
SM440	h ⁺ <i>leu1-32::rgf1-GFP:leu1⁺, nda3-KM311, rgf1::nat, leu1-32</i>
TE519	h ⁻ <i>cdc15-140, rlc1-tdTomato:natMX6, rgf1::his3⁺, leu1-32::rgf1-GFP:leu1⁺</i>
TE348	h ⁻ <i>cdc11-119, rlc1-tdTomato:natMX6, rgf1::kanMX6, leu1-32::rgf1-GFP:leu1⁺</i>
PG40	h ⁻ <i>rgf1::his3⁺, his3D1, ura4D18, leu1-32::rgf1-GFP:leu1⁺, ade6M210</i>
NG319	h ⁺ <i>cdc3-6, rgf1::his3⁺, his3D1, leu1-32::rgf1-GFP:leu1⁺</i>
TE149	h ⁻ <i>sid2-250, leu1-32::rgf1-GFP:leu1⁺, rgf1::natMX6</i>
SM213 ^a	h ⁺ <i>leu1-32, ura4d18</i>
SM341	h ⁺ <i>rgf1::natMX6, leu1-32, ura4D18</i>
YS864	h ⁺ <i>cdc4-8, leu1-32</i>
TE377	h ⁺ <i>cdc4-8, rgf1::kanMX6, leu1-32</i>
YS862	h ⁻ <i>rlc1::kanMX6, ura4D18, leu1-32, ade6M210</i>
TE389	h ⁺ <i>rlc1::kanMX6, rgf1::nat, ura4D18, leu1-32, ade6M210</i>
YS586 ^b	h ⁻ <i>cdc15-140, leu1-32</i>
NG203	h ⁻ <i>cdc15-140, rgf1::kanMX6</i>
TE246	h ⁺ <i>imp2::ura4⁺, leu1-32, ade6M210</i>
TE454	h ⁺ <i>imp2::ura4⁺, rgf1::natMX6, leu1-32</i>
YS865	h ⁺ <i>cdc12-112</i>
TE251	h ⁻ <i>cdc12-112, rgf1::natMX6</i>
TE478	h ⁻ <i>imp2-GFP:kanMX6, leu1:sid4-GFP, ura4D18, leu1-32</i>
TE495	h ⁻ <i>rgf1::natMX6, imp2-GFP:kanMX6, leu1:sid4-GFP, ura4D18, leu1-32</i>
TE249 ^c	h ⁺ <i>leu1::GFP-atb2:ura4⁺, rlc1-tdTomato:natMX6, leu1-32, ura4D18, his3D1</i>
TE257	h ⁺ <i>leu1::GFP-atb2:ura4⁺, rlc1-tdTomato:natMX6, rgf1::kanMX6, leu1-32, ura4D18</i>
TE470	h ⁺ <i>LactC2-GFP:natMX6, sad1-GFP:kanMX6, leu1-32, ura4D18, ade6M210</i>
TE472	h ⁺ <i>LactC2-GFP:natMX6, sad1-GFP:kanMX6, rgf1::natMX6, leu1-32, ura4D18, ade6M210</i>
TE399	h ⁺ <i>mEGFP-myo2:kanMX6, sid4-mCherry:hph, leu1-32, ura4D18</i>
TE402	h ⁺ <i>mEGFP-myo2:kanMX6, sid4-mCherry:hph, rgf1::natMX6, leu1-32, ura4D18</i>
TE450	h ⁺ <i>sad1-GFP:kanMX6, imp2-GFP:kanMX6, ura4D18</i>
TE452	h ⁺ <i>sad1-GFP:kanMX6, imp2-GFP:kanMX6, rgf1::natMX6, ura4D18</i>
TE491	h ⁻ <i>pmk1::ura4⁺, imp2-GFP:kanMX6, leu1:sid4-GFP, ura4D18, leu1-32</i>
TE585	h ⁻ <i>pmk1::ura4⁺, mEGFP-myo2:kanMX6, sid4-mcherry:hph, ura4D18</i>
TE545	h ⁻ <i>sty1::ura4⁺, imp2-GFP:kanMX6, leu1:sid4-GFP, ura4D18, leu1-32</i>
TE500	h ⁻ <i>pck2::kanMX6, imp2-GFP:kanMX6, leu1:sid4-GFP, ura4D18, leu1-32</i>
TE493	h ⁻ <i>pck1::kanMX6, imp2-GFP:kanMX6, leu1:sid4-GFP, ura4D18, leu1-32</i>
TE418	h ⁻ <i>rho2::natMX6, imp2-GFP:kanMX6, leu1:sid4-GFP, ura4D18, leu1-32</i>
TE580	h ⁻ <i>rho1-596:natMX6, imp2-GFP:kanMX6, leu1:sid4-GFP, ura4D18, leu1-32</i>
RC34	h ⁻ <i>leu1-32::rgf1-PTTR-GFP:leu1⁺, rlc1-tdTomato:natMX6, rgf1::kanMX6, sid4-mCherry:hph, leu1-32</i>
TE562	h ⁻ <i>cwg1-1, imp2-GFP:kanMX6, leu1:sid4-GFP, ura4D18, leu1-32</i>
TE564	h ⁻ <i>cwg1-1, pmk1::ura4⁺, imp2-GFP:kanMX6, leu1:sid4-GFP, ura4D18, leu1-32</i>
TE551 ^a	h ⁻ <i>pmk1::kanMX6, leu1-32, ura4D18, ade6M210</i>

Table 3 continued on next page

Table 3 continued

Strains	Genotypes
TE541	$h^- pmk1::ura4^+, hht1-RFP:kanMX6, imp2-GFP:kanMX6, leu1:sid4-GFP, ura4D18$
TE552	$h^- myp2::ura4^+, imp2-GFP:kanMX6, leu1:sid4-GFP, ura4D18, leu1-32$
TE615	$h^- rlc1::kanMX6, imp2-GFP:kanMX6, leu1:sid4-GFP, ura4D18, leu1-32$
TE513	$h^+ cdc7-GFP:ura4^+, sad1:dsRed:natMX6, ura4D18$
YS826	$h^+ sid2-GFP:ura4^+, leu1-32, ade6M210, ura4D18$
TE427	$h^+ sid2-GFP:ura4^+, rgf1::natMX6, leu1-32, ade6M210, ura4D18$
TE413	$h^+ cdc7-GFP:ura4^+, imp2-GFP:kanMX6$
TE414	$h^+ cdc7-GFP:ura4^+, imp2-GFP:kanMX6, rgf1::natMX6$
TE527	$h^+ clp1-GFP:kanMX6, imp2-GFP:kanMX6, leu1:sid4-GFP, leu1-32$
TE507	$h^- clp1::kanMX6, imp2-GFP:kanMX6, leu1:sid4-GFP, leu1-32$
EM352 ^d	$h^- pact1-LA:GFP:leu, ura4D18, leu1-32$
RC8	$h^- sid2-250, imp2-GFP:kanMX6, sfi1-GFP:kanMX6$
TE611	$h^- sid1-239, imp2-GFP:kanMX6, leu1:sid4-GFP, leu1-32$
YS1514	$h^- adf1-1, imp2-GFP:kanMX6, leu1:sid4-GFP, ura4D18, leu1-32$
TE592	$h^- cdc12-112, imp2-GFP:kanMX6, leu1:sid4-GFP, ura4D18, leu1-32$
TE591	$h^- pmk1::kanMX6, pmk1(K52E)-3 HA:leu1^+, imp2-GFP:kanMX6, sfi1-GFP:kanMX6, leu1-32$
PG323	$h^- pmk1-HA6h:ura4^+, his3D1, leu1-32$
YS5432	$h^- cwg1-1:natMX6, pmk1-HA6h:ura4^+$
TE261 ^a	$h^- cdc15-HA:kanMX6, ura4D18, leu1-32$
TE646	$h^- pmk1::ura4^+, cdc15-HA:kanMX6, ura4D18$
TE350	$h^- mid1-GFP:kanMX6, rlc1-tdTomato:natMX6, leu1-32, ura4D18, his3D1$
TE353	$h^- mid1-GFP:kanMX6, rlc1-tdTomato:natMX6, rgf1::his3^+, leu1-32, ura4D18, his3D1$
TE587	$h^- rgf1::natMX6, pmk1::ura4^+, imp2-GFP:kanMX6, leu1:sid4-GFP, ura4D18, leu1-32$

All strains were generated in this study except for strains with label^a from P. Perez (IBFG, University of Salamanca), label^b from H. Valdivieso (IBFG, University of Salamanca), label^c from J.C. Ribas (IBFG, University of Salamanca), label^d from M. Balasubramanian (University of Warwick).

(Schindelin et al., 2012). Super-resolution images were obtained using an Olympus IXplore SpinSR SoRa confocal Spinning disk microscope (Olympus), composed by the microscope Olympus IX83 (Olympus), U Plan Super Apochromatic 100x/1.45 oil immersion objective and sCMOS ORCA Flash 4.0 V3 camera (Hamamatsu).

Time-lapse imaging was carried out separately on two different microscopes: the previously described DeltaVision system and an Olympus IX81 spinning disk microscope (Olympus) equipped with a PlanApo 100x/1.40 oil immersion objective, a confocal CSUX1-A1 module (Yokogawa), and an Evolve (Photometrics) camera controlled by Metamorph software (Molecular Devices). One ml of midlog-phase cell cultures was collected by centrifugation (3500 g, 1 min) resuspended in 0.3 ml of YES containing the respective drugs and placed in a well of a μ -Slide eight well (Ibidi). Each of the wells was previously coated with 5 μ l of 1 mg/ml soybean lectin (Sigma-Aldrich). Cells were allowed to adhere to the bottom of the well for 2 min before removing the media. Then the cells were washed three times with media and resuspended in 0.3 ml of the same media. Time-lapse experiments were performed at 28°C. For imaging the temperature-sensitive strains at higher temperatures, the cells were shifted from 25°C to the described temperature and incubated for 1 hr prior to imaging. Using the DeltaVision system, 7 slices at 0.6 μ m were taken every 3 min within up to three different regions. With the spinning disk, 10 slices at 0.4 μ m were taken every 3 min in up to four regions in each of the four different wells.

In all time-lapse series, we used the SPB separation as time zero of the cellular clock. We define cytokinesis completion time as the time between the SPB separation and the complete closure of the AR. The time of the three stages of the CAR ring are defined as follows: assembly, from the appearance of nodes until there is a uniform ring signal; maturation, from a uniform ring signal to the start of its change in diameter; and constriction, from the first diameter change to its complete closure as a single point.

Total fluorescence of Cdc7p-GFP over time was measured using the sum projection of the slices taken in the spinning disk system. An area empty of cells was used to determine the average background fluorescence that was subtracted from the images. We used Sad1p-DsRed signal as a marker of both SPBs to select them with a 5-pixel diameter circle ($0.37 \mu\text{m}^2$), and we measured the total intensity of the green channel in these regions. Clp1-GFP nuclear intensity over time was measured using the sum projection of the slices taken in the DeltaVision system. An area empty of cells was used to determine the average background fluorescence that was subtracted from the images. Then, Sid4p-GFP was used as a marker of the SPBs to locate the nucleus, encircling it within a 42-pixel diameter circle ($6.14 \mu\text{m}^2$), which contained Sid4p in its periphery. The total intensity of the green channel in these regions was subsequently measured. The data were normalized according to their maximum and minimum.

Purification and detection of activated Pmk1

Cells from 30 ml of culture were harvested by centrifugation at 4°C , 500 g for 3 min, washed with cold PBS buffer, and immediately frozen in liquid nitrogen. Cell homogenates were prepared under native conditions employing chilled acid-washed glass beads and lysis buffer (10% glycerol, 50 mM Tris-HCl, pH 7.5, 150 mM NaCl, 0.1% Nonidet NP-40, plus a specific protease inhibitor cocktail: 100 M *p*-aminophenyl methanesulfonyl fluoride, leupeptin, and aprotinin). The lysates were cleared by centrifugation at 13,000 rpm for 15 min and Pmk1-HA6H was purified with Ni²⁺-NTA-agarose beads (Novagen). The purified proteins were loaded on 10% SDS-PAGE gels, transferred to an Immobilon-P membrane (Millipore), and incubated with either monoclonal mouse anti-HA (12CA5, Roche) or polyclonal rabbit anti-phospho-p42/44 antibodies (Cell Signaling). The immunoreactive bands were revealed with anti-mouse or anti-rabbit HRP secondary antibodies (Bio-Rad) and the ECL detection kit (Amersham Biosciences).

Western blot of synchronized cell cultures

Early-log phase cultures of cells containing Cdc15-HA were synchronized in S phase using hydroxyurea (HU) at a final concentration of 12.5 mM. After 4 hr of growth at 32°C HU was washed out and the cell cultures were released at 28°C , treated or untreated with BP (1 mg/ml). Samples were collected every 30 min after the first hour. 10 ml of cultures were mixed with 40 ml of 50 mM Tris-HCl pH 7. Cells were immediately harvested by centrifugation at 4°C , 500 g for 3 min and frozen at -80°C in 100 ml of 20% TCA. Protein extracts were obtained by TCA precipitation. Proteins were resolved with 7% SDS-PAGE gels, transferred to an Immobilon-P membrane (Millipore), incubated with monoclonal mouse anti-HA antibodies (12CA5, Roche) and revealed with anti-mouse HRP secondary antibodies (Bio-Rad) and the ECL detection kit (Amersham Biosciences).

Acknowledgements

We wish to thank Cesar Roncero and Henar Valdivieso for their support and our colleges from the Cell Wall group of the Institute of Functional Biology and Genomics at the University Salamanca. Special thanks to Sergio Rincon for his very helpful comments on the manuscript and Carmen Castro for help with microscopy. The English text was revised by E Keck. T Edreira and E Manjon were financially supported by a contract obtained through the Regional Government of Castile and Leon, co-financed by the European Social Fund. R Celador was financially supported by a collaboration grant from the University of Salamanca. Funding sources: MEIC, Spain (BFU2017-84508-P; Regional Government of Castile and Leon [SA073U14]). Funding for open access charge: MEIC.

Additional information

Funding

Funder	Grant reference number	Author
Regional Government of Castile and Leon	The European Social Fund	Tomás Edreira Elvira Manjón
University of Salamanca		Rubén Celador

The funders had no role in study design, data collection and interpretation, or the decision to submit the work for publication.

Author contributions

Tomás Edreira, Conceptualization, Formal analysis, Validation, Investigation, Methodology, Writing - review and editing; Rubén Celador, Conceptualization, Formal analysis, Validation, Investigation, Methodology; Elvira Manjón, Supervision, Validation, Investigation, Methodology; Yolanda Sánchez, Conceptualization, Formal analysis, Supervision, Funding acquisition, Investigation, Writing - original draft, Writing - review and editing

Author ORCIDs

Tomás Edreira  <https://orcid.org/0000-0002-1985-0940>

Yolanda Sánchez  <https://orcid.org/0000-0002-7650-9319>

Decision letter and Author response

Decision letter <https://doi.org/10.7554/eLife.59333.sa1>

Author response <https://doi.org/10.7554/eLife.59333.sa2>

Additional files

Supplementary files

- Transparent reporting form

Data availability

All data generated or analysed during this study are included in the manuscript and supporting files.

References

- Aguilar-Zapata D**, Petraitiene R, Petraitis V. 2015. Echinocandins: the expanding antifungal armamentarium. *Clinical Infectious Diseases* **61 Suppl 6**:S604–S611. DOI: <https://doi.org/10.1093/cid/civ814>, PMID: 26567277
- Akamatsu M**, Berro J, Pu KM, Tebbs IR, Pollard TD. 2014. Cytokinetic nodes in fission yeast arise from two distinct types of nodes that merge during interphase. *Journal of Cell Biology* **204**:977–988. DOI: <https://doi.org/10.1083/jcb.201307174>, PMID: 24637325
- Alcaide-Gavilán M**, Lahoz A, Daga RR, Jimenez J. 2014. Feedback regulation of SIN by Etd1 and Rho1 in fission yeast. *Genetics* **196**:455–470. DOI: <https://doi.org/10.1534/genetics.113.155218>, PMID: 24336750
- Almonacid M**, Celton-Morizur S, Jakubowski JL, Dingli F, Loew D, Mayeux A, Chen JS, Gould KL, Clifford DM, Paoletti A. 2011. Temporal control of contractile ring assembly by Plo1 regulation of myosin II recruitment by Mid1/anillin. *Current Biology* **21**:473–479. DOI: <https://doi.org/10.1016/j.cub.2011.02.003>, PMID: 21376600
- Arasada R**, Pollard TD. 2014. Contractile ring stability in *S. pombe* depends on F-BAR protein Cdc15p and Bgs1p transport from the golgi complex. *Cell Reports* **8**:1533–1544. DOI: <https://doi.org/10.1016/j.celrep.2014.07.048>, PMID: 25159149
- Bähler J**, Steever AB, Wheatley S, Wang Y, Pringle JR, Gould KL, McCollum D. 1998. Role of polo kinase and Mid1p in determining the site of cell division in fission yeast. *Journal of Cell Biology* **143**:1603–1616. DOI: <https://doi.org/10.1083/jcb.143.6.1603>, PMID: 9852154
- Bähler J**. 2005. A Transcriptional Pathway for Cell Separation in Fission Yeast. *Cell Cycle* **4**:39–41. DOI: <https://doi.org/10.4161/cc.4.1.1336>
- Barba G**, Soto T, Madrid M, Núñez A, Vicente J, Gacto M, Cansado J, Yeast Physiology G. 2008. Activation of the cell integrity pathway is channelled through diverse signalling elements in fission yeast. *Cellular Signalling* **20**:748–757. DOI: <https://doi.org/10.1016/j.cellsig.2007.12.017>

- Bohnert KA**, Gould KL. 2012. Cytokinesis-based constraints on polarized cell growth in fission yeast. *PLoS Genetics* **8**:e1003004. DOI: <https://doi.org/10.1371/journal.pgen.1003004>, PMID: 23093943
- Celton-Morizur S**, Bordes N, Fraiser V, Tran PT, Paoletti A. 2004. C-Terminal anchoring of mid1p to membranes stabilizes cytokinetic ring position in early mitosis in fission yeast. *Molecular and Cellular Biology* **24**:10621–10635. DOI: <https://doi.org/10.1128/MCB.24.24.10621-10635.2004>, PMID: 15572668
- Chang F**, Drubin D, Nurse P. 1997. cdc12p, a protein required for cytokinesis in fission yeast, is a component of the cell division ring and interacts with profilin. *Journal of Cell Biology* **137**:169–182. DOI: <https://doi.org/10.1083/jcb.137.1.169>, PMID: 9105045
- Cheffings TH**, Burroughs NJ, Balasubramanian MK. 2016. Actomyosin ring formation and tension generation in eukaryotic cytokinesis. *Current Biology* **26**:R719–R737. DOI: <https://doi.org/10.1016/j.cub.2016.06.071>, PMID: 27505246
- Chen D**, Toone WM, Mata J, Lyne R, Burns G, Kivinen K, Brazma A, Jones N, Bähler J. 2003. Global transcriptional responses of fission yeast to environmental stress. *Molecular Biology of the Cell* **14**:214–229. DOI: <https://doi.org/10.1091/mbc.e02-08-0499>, PMID: 12529438
- Chen CT**, Feoktistova A, Chen JS, Shim YS, Clifford DM, Gould KL, McCollum D. 2008a. The SIN kinase Sid2 regulates cytoplasmic retention of the *S. pombe* Cdc14-like phosphatase Clp1. *Current Biology* **18**:1594–1599. DOI: <https://doi.org/10.1016/j.cub.2008.08.067>, PMID: 18951025
- Chen D**, Wilkinson CR, Watt S, Penkett CJ, Toone WM, Jones N, Bähler J. 2008b. Multiple pathways differentially regulate global oxidative stress responses in fission yeast. *Molecular Biology of the Cell* **19**:308–317. DOI: <https://doi.org/10.1091/mbc.e07-08-0735>, PMID: 18003976
- Chen Q**, Pollard TD. 2011. Actin filament severing by cofilin is more important for assembly than constriction of the cytokinetic contractile ring. *Journal of Cell Biology* **195**:485–498. DOI: <https://doi.org/10.1083/jcb.201103067>, PMID: 22024167
- Clifford DM**, Wolfe BA, Roberts-Galbraith RH, McDonald WH, Yates JR, Gould KL. 2008. The Clp1/Cdc14 phosphatase contributes to the robustness of cytokinesis by association with anillin-related Mid1. *Journal of Cell Biology* **181**:79–88. DOI: <https://doi.org/10.1083/jcb.200709060>, PMID: 18378776
- Coffman VC**, Sees JA, Kovar DR, Wu JQ. 2013. The formins Cdc12 and For3 cooperate during contractile ring assembly in cytokinesis. *Journal of Cell Biology* **203**:101–114. DOI: <https://doi.org/10.1083/jcb.201305022>, PMID: 24127216
- Cortés JC**, Carnero E, Ishiguro J, Sánchez Y, Durán A, Ribas JC. 2005. The novel fission yeast (1,3)beta-D-glucan synthase catalytic subunit Bgs4p is essential during both cytokinesis and polarized growth. *Journal of Cell Science* **118**:157–174. DOI: <https://doi.org/10.1242/jcs.01585>, PMID: 15615781
- Cortés JCG**, Konomi M, Martins IM, Muñoz J, Moreno MB, Osumi M, Durán A, Ribas JC. 2007. The (1,3)β-d-glucan synthase subunit Bgs1p is responsible for the fission yeast primary septum formation. *Molecular Microbiology* **65**:201–217. DOI: <https://doi.org/10.1111/j.1365-2958.2007.05784.x>
- D'Avino PP**, Giansanti MG, Petronczki M. 2015. Cytokinesis in animal cells. *Cold Spring Harbor Perspectives in Biology* **7**:a015834. DOI: <https://doi.org/10.1101/cshperspect.a015834>, PMID: 25680833
- Dey SK**, Pollard TD. 2018. Involvement of the septation initiation network in events during cytokinesis in fission yeast. *Journal of Cell Science* **131**:jcs216895. DOI: <https://doi.org/10.1242/jcs.216895>, PMID: 30072443
- Fankhauser C**, Reymond A, Cerutti L, Utzig S, Hofmann K, Simanis V. 1995. The *S. pombe* cdc15 gene is a key element in the reorganization of F-actin at mitosis. *Cell* **82**:435–444. DOI: [https://doi.org/10.1016/0092-8674\(95\)90432-8](https://doi.org/10.1016/0092-8674(95)90432-8), PMID: 7634333
- Feoktistova A**, Morrell-Falvey J, Chen J-S, Singh NS, Balasubramanian MK, Gould KL. 2012. The fission yeast septation initiation network (SIN) kinase, Sid2, is required for SIN asymmetry and regulates the SIN scaffold, Cdc11. *Molecular Biology of the Cell* **23**:1636–1645. DOI: <https://doi.org/10.1091/mbc.e11-09-0792>
- Forsburg SL**, Rhind N. 2006. Basic methods for fission yeast. *Yeast* **23**:173–183. DOI: <https://doi.org/10.1002/yea.1347>, PMID: 16498704
- G Cortés JC**, Ramos M, Konomi M, Barragán I, Moreno MB, Alcaide-Gavilán M, Moreno S, Osumi M, Pérez P, Ribas JC. 2018. Specific detection of fission yeast primary septum reveals septum and cleavage furrow ingression during early anaphase independent of mitosis completion. *PLoS Genetics* **14**:e1007388. DOI: <https://doi.org/10.1371/journal.pgen.1007388>, PMID: 29813053
- Ganem NJ**, Storchova Z, Pellman D. 2007. Tetraploidy, aneuploidy and cancer. *Current Opinion in Genetics & Development* **17**:157–162. DOI: <https://doi.org/10.1016/j.gde.2007.02.011>, PMID: 17324569
- García P**, Tajadura V, García I, Sánchez Y. 2006a. Rgf1p is a specific Rho1-GEF that coordinates cell polarization with cell wall biogenesis in fission yeast. *Molecular Biology of the Cell* **17**:1620–1631. DOI: <https://doi.org/10.1091/mbc.e05-10-0933>, PMID: 16421249
- García P**, Tajadura V, García I, Sánchez Y. 2006b. Role of rho GTPases and Rho-GEFs in the regulation of cell shape and integrity in fission yeast. *Yeast* **23**:1031–1043. DOI: <https://doi.org/10.1002/yea.1409>, PMID: 17072882
- García P**, Tajadura V, Sanchez Y. 2009a. The Rho1p exchange factor Rgf1p signals upstream from the Pmk1 mitogen-activated protein kinase pathway in fission yeast. *Molecular Biology of the Cell* **20**:721–731. DOI: <https://doi.org/10.1091/mbc.e08-07-0673>, PMID: 19037094
- García P**, García I, Marcos F, de Garibay GR, Sánchez Y. 2009b. Fission yeast rgf2p is a rho1p guanine nucleotide exchange factor required for spore wall maturation and for the maintenance of cell integrity in the absence of rgf1p. *Genetics* **181**:1321–1334. DOI: <https://doi.org/10.1534/genetics.108.094839>, PMID: 19189958

- García Cortés JC**, Ramos M, Osumi M, Pérez P, Ribas JC. 2016. The cell biology of fission yeast septation. *Microbiology and Molecular Biology Reviews* **80**:779–791. DOI: <https://doi.org/10.1128/MMBR.00013-16>, PMID: 27466282
- Glotzer M**. 2017. Cytokinesis in metazoa and fungi. Cold Spring Harbor Perspectives in Biology. DOI: <https://doi.org/10.1101/cshperspect.a022343>
- Goss JW**, Kim S, Bledsoe H, Pollard TD. 2014. Characterization of the roles of Blt1p in fission yeast cytokinesis. *Molecular Biology of the Cell* **25**:1946–1957. DOI: <https://doi.org/10.1091/mbc.e13-06-0300>, PMID: 24790095
- Goyal A**, Takaine M, Simanis V, Nakano K. 2011. Dividing the spoils of growth and the cell cycle: The fission yeast as a model for the study of cytokinesis. *Cytoskeleton* **68**:69–88. DOI: <https://doi.org/10.1002/cm.20500>
- Grallert A**, Connolly Y, Smith DL, Simanis V, Hagan IM. 2012. The *S. pombe* cytokinesis NDR kinase Sid2 activates Fin1 NIMA kinase to control mitotic commitment through Pom1/Wee1. *Nature Cell Biology* **14**:738–745. DOI: <https://doi.org/10.1038/ncb2514>
- Gupta S**, Mana-Capelli S, McLean JR, Chen C-T, Ray S, Gould KL, McCollum D. 2013. Identification of SIN Pathway Targets Reveals Mechanisms of Crosstalk between NDR Kinase Pathways. *Current Biology* **23**:333–338. DOI: <https://doi.org/10.1016/j.cub.2013.01.014>
- Hiraoka Y**, Toda T, Yanagida M. 1984. The *NDA3* gene of fission yeast encodes β -tubulin: a cold-sensitive *nda3* mutation reversibly blocks spindle formation and chromosome movement in mitosis. *Cell* **39**:349–358. DOI: [https://doi.org/10.1016/0092-8674\(84\)90013-8](https://doi.org/10.1016/0092-8674(84)90013-8), PMID: 6094012
- Huang J**, Huang Y, Yu H, Subramanian D, Padmanabhan A, Thadani R, Tao Y, Tang X, Wedlich-Soldner R, Balasubramanian MK. 2012. Nonmedially assembled F-actin cables incorporate into the actomyosin ring in fission yeast. *Journal of Cell Biology* **199**:831–847. DOI: <https://doi.org/10.1083/jcb.201209044>
- Jin QW**, Zhou M, Bimbo A, Balasubramanian MK, McCollum D. 2006. A role for the septation initiation network in septum assembly revealed by genetic analysis of *sid2-250* suppressors. *Genetics* **172**:2101–2112. DOI: <https://doi.org/10.1534/genetics.105.050955>, PMID: 16415366
- Johnson AE**, McCollum D, Gould KL. 2012. Polar opposites: fine-tuning cytokinesis through SIN asymmetry. *Cytoskeleton* **69**:686–699. DOI: <https://doi.org/10.1002/cm.21044>, PMID: 22786806
- Kamasaki T**, Osumi M, Mabuchi I. 2007. Three-dimensional arrangement of F-actin in the contractile ring of fission yeast. *Journal of Cell Biology* **178**:765–771. DOI: <https://doi.org/10.1083/jcb.200612018>, PMID: 17724118
- Kühn S**, Geyer M. 2014. Formins as effector proteins of rho GTPases. *Small GTPases* **5**:e983876. DOI: <https://doi.org/10.4161/sgtp.29513>
- Kuranda K**, Leberre V, Sokol S, Palamarczyk G, Francois J. 2006. Investigating the caffeine effects in the yeast *Saccharomyces cerevisiae* brings new insights into the connection between TOR, PKC and ras/cAMP signalling pathways. *Molecular Microbiology* **61**:1147–1166. DOI: <https://doi.org/10.1111/j.1365-2958.2006.05300.x>
- Laplante C**, Berro J, Karatekin E, Hernandez-Leyva A, Lee R, Pollard TD. 2015. Three myosins contribute uniquely to the assembly and constriction of the fission yeast cytokinetic contractile ring. *Current Biology* **25**:1955–1965. DOI: <https://doi.org/10.1016/j.cub.2015.06.018>, PMID: 26144970
- Laporte D**, Coffman VC, Lee IJ, Wu JQ. 2011. Assembly and architecture of precursor nodes during fission yeast cytokinesis. *Journal of Cell Biology* **192**:1005–1021. DOI: <https://doi.org/10.1083/jcb.201008171>, PMID: 21422229
- Le Goff X**, Woollard A, Simanis V. 1999. Analysis of the *cps1* gene provides evidence for a septation checkpoint in *Schizosaccharomyces pombe*. *Molecular and General Genetics MGG* **262**:163–172. DOI: <https://doi.org/10.1007/s004380051071>, PMID: 10503548
- Le Goff X**, Motegi F, Salimova E, Mabuchi I, Simanis V. 2000. The *S. pombe* *rlc1* gene encodes a putative myosin regulatory light chain that binds the type II myosins *myo3p* and *myo2p*. *Journal of Cell Science* **113**:4157–4163. PMID: 11069761
- Liu J**, Wang H, Balasubramanian MK. 2000. A checkpoint that monitors cytokinesis in *Schizosaccharomyces pombe*. *Journal of Cell Science* **113**:1223–1230. PMID: 10704373
- Loewith R**, Hubberstey A, Young D. 2000. Skh1, the MEK component of the *mkh1* signaling pathway in *Schizosaccharomyces pombe*. *Journal of Cell Science* **113**:153–160. PMID: 10591634
- Lord M**, Laves E, Pollard TD. 2005. Cytokinesis depends on the motor domains of myosin-II in fission yeast but not in budding yeast. *Molecular Biology of the Cell* **16**:5346–5355. DOI: <https://doi.org/10.1091/mbc.e05-07-0601>, PMID: 16148042
- Ma Y**, Kuno T, Kita A, Asayama Y, Sugiura R. 2006. Rho2 is a target of the farnesyltransferase Cpp1 and acts upstream of Pmk1 mitogen-activated protein kinase signaling in fission yeast. *Molecular Biology of the Cell* **17**:5028–5037. DOI: <https://doi.org/10.1091/mbc.e06-08-0688>, PMID: 17005909
- Madrid M**, Soto T, Khong HK, Franco A, Vicente J, Pérez P, Gacto M, Cansado J. 2006. Stress-induced response, localization, and regulation of the Pmk1 cell integrity pathway in *Schizosaccharomyces pombe*. *Journal of Biological Chemistry* **281**:2033–2043. DOI: <https://doi.org/10.1074/jbc.M506467200>, PMID: 16291757
- Madrid M**, Núñez A, Soto T, Vicente-Soler J, Gacto M, Cansado J. 2007. Stress-activated protein kinase-mediated down-regulation of the cell integrity pathway mitogen-activated protein kinase Pmk1p by protein phosphatases. *Molecular Biology of the Cell* **18**:4405–4419. DOI: <https://doi.org/10.1091/mbc.e07-05-0484>, PMID: 17761528
- Madrid M**, Jiménez R, Sánchez-Mir L, Soto T, Franco A, Vicente-Soler J, Gacto M, Pérez P, Cansado J. 2015. Multiple layers of regulation influence cell integrity control by the PKC ortholog Pck2 in fission yeast. *Journal of Cell Science* **128**:266–280. DOI: <https://doi.org/10.1242/jcs.158295>, PMID: 25416816

- Mana-Capelli S**, McLean JR, Chen CT, Gould KL, McCollum D. 2012. The kinesin-14 Klp2 is negatively regulated by the SIN for proper spindle elongation and telophase nuclear positioning. *Molecular Biology of the Cell* **23**: 4592–4600. DOI: <https://doi.org/10.1091/mbc.e12-07-0532>, PMID: 23087209
- McDonald NA**, Lind AL, Smith SE, Li R, Gould KL. 2017. Nanoscale architecture of the *Schizosaccharomyces pombe* contractile ring. *eLife* **6**:e28865. DOI: <https://doi.org/10.7554/eLife.28865>, PMID: 28914606
- Meitinger F**, Palani S. 2016. Actomyosin ring driven cytokinesis in budding yeast. *Seminars in Cell & Developmental Biology* **53**:19–27. DOI: <https://doi.org/10.1016/j.semcdb.2016.01.043>, PMID: 26845196
- Mendes Pinto I**, Rubinstein B, Kucharavy A, Unruh JR, Li R. 2012. Actin depolymerization drives actomyosin ring contraction during budding yeast cytokinesis. *Developmental Cell* **22**:1247–1260. DOI: <https://doi.org/10.1016/j.devcel.2012.04.015>, PMID: 22698284
- Mishra M**, Karagiannis J, Trautmann S, Wang H, McCollum D, Balasubramanian MK. 2004. The Clp1p/Flp1p phosphatase ensures completion of cytokinesis in response to minor perturbation of the cell division machinery in *Schizosaccharomyces pombe*. *Journal of Cell Science* **117**:3897–3910. DOI: <https://doi.org/10.1242/jcs.01244>, PMID: 15265986
- Mishra M**, Karagiannis J, Sevugan M, Singh P, Balasubramanian MK. 2005. The 14-3-3 protein Rad24p modulates function of the Cdc14p family phosphatase Clp1p/Flp1p in fission yeast. *Current Biology : CB* **15**:1376–1383. DOI: <https://doi.org/10.1016/j.cub.2005.06.070>, PMID: 16085489
- Mishra M**, Kashiwazaki J, Takagi T, Srinivasan R, Huang Y, Balasubramanian MK, Mabuchi I. 2013. In vitro contraction of cytokinetic ring depends on myosin II but not on actin dynamics. *Nature Cell Biology* **15**:853–859. DOI: <https://doi.org/10.1038/ncb2781>, PMID: 23770677
- Moreno S**, Klar A, Nurse P. 1991. Molecular genetic analysis of fission yeast *Schizosaccharomyces pombe*. *Meth. Enzymol* **194**:795–823. DOI: [https://doi.org/10.1016/0076-6879\(91\)94059-L](https://doi.org/10.1016/0076-6879(91)94059-L)
- Morrell-Falvey JL**, Ren L, Feoktistova A, Haese GD, Gould KL. 2005. Cell wall remodeling at the fission yeast cell division site requires the Rho-GEF Rgf3p. *Journal of Cell Science* **118**:5563–5573. DOI: <https://doi.org/10.1242/jcs.02664>, PMID: 16291723
- Moseley JB**, Mayeux A, Paoletti A, Nurse P. 2009. A spatial gradient coordinates cell size and mitotic entry in fission yeast. *Nature* **459**:857–860. DOI: <https://doi.org/10.1038/nature08074>
- Muñoz J**, Cortés JC, Sipiczki M, Ramos M, Clemente-Ramos JA, Moreno MB, Martins IM, Pérez P, Ribas JC. 2013. Extracellular cell wall $\beta(1,3)$ glucan is required to couple septation to actomyosin ring contraction. *Journal of Cell Biology* **203**:265–282. DOI: <https://doi.org/10.1083/jcb.201304132>, PMID: 24165938
- Muñoz S**, Manjón E, García P, Sunnerhagen P, Sánchez Y. 2014. The checkpoint-dependent nuclear accumulation of Rho1p exchange factor Rgf1p is important for tolerance to chronic replication stress. *Molecular Biology of the Cell* **25**:1137–1150. DOI: <https://doi.org/10.1091/mbc.e13-11-0689>, PMID: 24478458
- Mutoh T**, Nakano K, Mabuchi I. 2005. Rho1-GEFs Rgf1 and Rgf2 are involved in formation of cell wall and septum, while Rgf3 is involved in cytokinesis in fission yeast. *Genes to Cells* **10**:1189–1202. DOI: <https://doi.org/10.1111/j.1365-2443.2005.00908.x>, PMID: 16324155
- Nähse V**, Christ L, Stenmark H, Campsteijn C. 2017. The abscission checkpoint: making it to the final cut. *Trends in Cell Biology* **27**:1–11. DOI: <https://doi.org/10.1016/j.tcb.2016.10.001>, PMID: 27810282
- Nakano K**, Arai R, Mabuchi I. 1997. The small GTP-binding protein Rho1 is a multifunctional protein that regulates actin localization, cell polarity, and septum formation in the fission yeast *Schizosaccharomyces pombe*. *Genes to Cells* **2**:679–694. DOI: <https://doi.org/10.1046/j.1365-2443.1997.1540352.x>, PMID: 9491802
- Nakano K**, Mabuchi I. 2006. Actin-depolymerizing protein Adf1 is required for formation and maintenance of the contractile ring during cytokinesis in fission yeast. *Molecular Biology of the Cell* **17**:1933–1945. DOI: <https://doi.org/10.1091/mbc.e05-09-0900>, PMID: 16467379
- Normand G**, King RW. 2010. Understanding cytokinesis failure. *Advances in Experimental Medicine and Biology* **676**:27–55. DOI: https://doi.org/10.1007/978-1-4419-6199-0_3, PMID: 20687468
- Okada H**, Wloka C, Wu JQ, Bi E. 2019. Distinct roles of Myosin-II isoforms in cytokinesis under normal and stressed conditions. *iScience* **14**:69–87. DOI: <https://doi.org/10.1016/j.isci.2019.03.014>, PMID: 30928696
- Padmanabhan A**, Bakka K, Sevugan M, Naqvi NI, D'souza V, Tang X, Mishra M, Balasubramanian MK. 2011. IQGAP-Related Rng2p Organizes Cortical Nodes and Ensures Position of Cell Division in Fission Yeast. *Current Biology* **21**:467–472. DOI: <https://doi.org/10.1016/j.cub.2011.01.059>
- Palani S**, Chew TG, Ramanujam S, Kamnev A, Harne S, Chapa-Y-Lazo B, Hogg R, Sevugan M, Mishra M, Gayathri P, Balasubramanian MK. 2017. Motor activity dependent and independent functions of myosin II contribute to actomyosin ring assembly and contraction in *Schizosaccharomyces pombe*. *Current Biology* **27**:751–757. DOI: <https://doi.org/10.1016/j.cub.2017.01.028>, PMID: 28238661
- Pelham RJ**, Chang F. 2002. Actin dynamics in the contractile ring during cytokinesis in fission yeast. *Nature* **419**: 82–86. DOI: <https://doi.org/10.1038/nature00999>, PMID: 12214236
- Pérez P**, Cortés JC, Martín-García R, Ribas JC. 2016. Overview of fission yeast septation. *Cellular Microbiology* **18**:1201–1207. DOI: <https://doi.org/10.1111/cmi.12611>, PMID: 27155541
- Pérez P**, Cansado J. 2010a. Cell integrity signaling and response to stress in fission yeast. *Current Protein & Peptide Science* **11**:680–692. DOI: <https://doi.org/10.2174/138920310794557718>, PMID: 21235504
- Pérez P**, Rincón SA. 2010b. Rho GTPases: regulation of cell polarity and growth in yeasts. *Biochemical Journal* **426**:243–253. DOI: <https://doi.org/10.1042/BJ20091823>, PMID: 20175747
- Petersen J**, Hagan IM. 2005. Polo kinase links the stress pathway to cell cycle control and tip growth in fission yeast. *Nature* **435**:507–512. DOI: <https://doi.org/10.1038/nature03590>, PMID: 15917811

- Petersen J, Nurse P. 2007. TOR signalling regulates mitotic commitment through the stress MAP kinase pathway and the polo and Cdc2 kinases. *Nature Cell Biology* **9**:1263–1272. DOI: <https://doi.org/10.1038/ncb1646>, PMID: 17952063
- Plouffe SW, Meng Z, Lin KC, Lin B, Hong AW, Chun JV, Guan K-L. 2016. Characterization of Hippo Pathway Components by Gene Inactivation. *Molecular Cell* **64**:993–1008. DOI: <https://doi.org/10.1016/j.molcel.2016.10.034>
- Pollard TD. 2017. Nine unanswered questions about cytokinesis. *Journal of Cell Biology* **216**:3007–3016. DOI: <https://doi.org/10.1083/jcb.201612068>, PMID: 28807993
- Pollard TD, Wu JQ. 2010. Understanding cytokinesis: lessons from fission yeast. *Nature Reviews Molecular Cell Biology* **11**:149–155. DOI: <https://doi.org/10.1038/nrm2834>, PMID: 20094054
- Proctor SA, Minc N, Boudaoud A, Chang F. 2012. Contributions of turgor pressure, the contractile ring, and septum assembly to forces in cytokinesis in fission yeast. *Current Biology* **22**:1601–1608. DOI: <https://doi.org/10.1016/j.cub.2012.06.042>, PMID: 22840513
- Ren L, Willet AH, Roberts-Galbraith RH, McDonald NA, Feoktistova A, Chen J-S, Huang H, Guillen R, Boone C, Sidhu SS, Beckley JR, Gould KL. 2015. The Cdc15 and Imp2 SH3 domains cooperatively scaffold a network of proteins that redundantly ensure efficient cell division in fission yeast. *Molecular Biology of the Cell* **26**:256–269. DOI: <https://doi.org/10.1091/mbc.E14-10-1451>
- Rincon SA, Estravis M, Dingli F, Loew D, Tran PT, Paoletti A. 2017. SIN-Dependent dissociation of the SAD kinase Cdr2 from the cell cortex resets the Division plane. *Current Biology* **27**:534–542. DOI: <https://doi.org/10.1016/j.cub.2016.12.050>, PMID: 28162898
- Rincon SA, Paoletti A. 2016. Molecular control of fission yeast cytokinesis. *Seminars in Cell & Developmental Biology* **53**:28–38. DOI: <https://doi.org/10.1016/j.semcdb.2016.01.007>, PMID: 26806637
- Roberts-Galbraith RH, Chen JS, Wang J, Gould KL. 2009. The SH3 domains of two PCH family members cooperate in assembly of the *Schizosaccharomyces pombe* contractile ring. *Journal of Cell Biology* **184**:113–127. DOI: <https://doi.org/10.1083/jcb.200806044>, PMID: 19139265
- Roberts-Galbraith RH, Ohi MD, Ballif BA, Chen JS, McLeod I, McDonald WH, Gygi SP, Yates JR, Gould KL. 2010. Dephosphorylation of F-BAR protein Cdc15 modulates its conformation and stimulates its scaffolding activity at the cell division site. *Molecular Cell* **39**:86–99. DOI: <https://doi.org/10.1016/j.molcel.2010.06.012>, PMID: 20603077
- Roncero C, Sánchez Y. 2010. Cell separation and the maintenance of cell integrity during cytokinesis in yeast: the assembly of a septum. *Yeast* **27**:521–530. DOI: <https://doi.org/10.1002/yea.1779>, PMID: 20641019
- Sánchez-Mir L, Franco A, Madrid M, Vicente-Soler J, Villar-Tajadura MA, Soto T, Pérez P, Gacto M, Cansado J. 2012. Biological significance of nuclear localization of mitogen-activated protein kinase Pmk1 in fission yeast. *Journal of Biological Chemistry* **287**:26038–26051. DOI: <https://doi.org/10.1074/jbc.M112.345611>, PMID: 22685296
- Sánchez-Mir L, Franco A, Martín-García R, Madrid M, Vicente-Soler J, Soto T, Gacto M, Pérez P, Cansado J. 2014a. Rho2 palmitoylation is required for plasma membrane localization and proper signaling to the fission yeast cell integrity mitogen-activated protein kinase pathway. *Molecular and Cellular Biology* **34**:2745–2759. DOI: <https://doi.org/10.1128/MCB.01515-13>, PMID: 24820419
- Sánchez-Mir L, Soto T, Franco A, Madrid M, Viana RA, Vicente J, Gacto M, Pérez P, Cansado J. 2014b. Rho1 GTPase and PKC ortholog Pck1 are upstream activators of the cell integrity MAPK pathway in fission yeast. *PLoS ONE* **9**:e88020. DOI: <https://doi.org/10.1371/journal.pone.0088020>, PMID: 24498240
- Schindelin J, Arganda-Carreras I, Frise E, Kaynig V, Longair M, Pietzsch T, Preibisch S, Rueden C, Saalfeld S, Schmid B, Tinevez JY, White DJ, Hartenstein V, Eliceiri K, Tomancak P, Cardona A. 2012. Fiji: an open-source platform for biological-image analysis. *Nature Methods* **9**:676–682. DOI: <https://doi.org/10.1038/nmeth.2019>, PMID: 22743772
- Sengar AS, Markley NA, Marini NJ, Young D. 1997. Mkh1, a MEK kinase required for cell wall integrity and proper response to osmotic and temperature stress in *Schizosaccharomyces pombe*. *Molecular and Cellular Biology* **17**:3508–3519. DOI: <https://doi.org/10.1128/MCB.17.7.3508>, PMID: 9199286
- Simanis V. 2015. *Pombe's* thirteen - control of fission yeast cell division by the septation initiation network. *Journal of Cell Science* **128**:1465–1474. DOI: <https://doi.org/10.1242/jcs.094821>, PMID: 25690009
- Sladewski TE, Previs MJ, Lord M. 2009. Regulation of fission yeast myosin-II function and contractile ring dynamics by regulatory light-chain and heavy-chain phosphorylation. *Molecular Biology of the Cell* **20**:3941–3952. DOI: <https://doi.org/10.1091/mbc.e09-04-0346>, PMID: 19570908
- Slubowski CJ, Funk AD, Roesner JM, Paulissen SM, Huang LS. 2015. Plasmids for C-terminal tagging in *Saccharomyces cerevisiae* that contain improved GFP proteins, envy and ivy. *Yeast* **32**:379–387. DOI: <https://doi.org/10.1002/yea.3065>, PMID: 25612242
- Sohrmann M, Fankhauser C, Brodbeck C, Simanis V. 1996. The dmf1/mid1 gene is essential for correct positioning of the division septum in fission yeast. *Genes & Development* **10**:2707–2719. DOI: <https://doi.org/10.1101/gad.10.21.2707>, PMID: 8946912
- Stachowiak MR, Laplante C, Chin HF, Guirao B, Karatekin E, Pollard TD, O'Shaughnessy B. 2014. Mechanism of cytokinetic contractile ring constriction in fission yeast. *Developmental Cell* **29**:547–561. DOI: <https://doi.org/10.1016/j.devcel.2014.04.021>, PMID: 24914559
- Sugiura R, Toda T, Shuntoh H, Yanagida M, Kuno T. 1998. *pmp1+*, a suppressor of calcineurin deficiency, encodes a protein similar to the *cdc10+* and *SWI4* gene products. *The EMBO Journal* **17**:140–148.

- Tajadura V**, García B, García I, García P, Sánchez Y. 2004. *Schizosaccharomyces pombe* Rgf3p is a specific Rho1 GEF that regulates cell wall beta-glucan biosynthesis through the GTPase Rho1p. *Journal of Cell Science* **117**: 6163–6174. DOI: <https://doi.org/10.1242/jcs.01530>, PMID: 15546915
- Takada H**, Nishimura M, Asayama Y, Mannse Y, Ishiwata S, Kita A, Doi A, Nishida A, Kai N, Moriuchi S, Tohda H, Giga-Hama Y, Kuno T, Sugiura R. 2007. Atf1 is a target of the mitogen-activated protein kinase Pmk1 and regulates cell integrity in fission yeast. *Molecular Biology of the Cell* **18**:4794–4802. DOI: <https://doi.org/10.1091/mbc.e07-03-0282>, PMID: 17881729
- Thiyagarajan S**, Munteanu EL, Arasada R, Pollard TD, O’Shaughnessy B. 2015. The fission yeast cytokinetic contractile ring regulates septum shape and closure. *Journal of Cell Science* **128**:3672–3681. DOI: <https://doi.org/10.1242/jcs.166926>, PMID: 26240178
- Toda T**, Dhut S, Superti-Furga G, Gotoh Y, Nishida E, Sugiura R, Kuno T. 1996. The fission yeast pmk1⁺ gene encodes a novel mitogen-activated protein kinase homolog which regulates cell integrity and functions coordinately with the protein kinase C pathway. *Molecular and Cellular Biology* **16**:6752–6764. DOI: <https://doi.org/10.1128/MCB.16.12.6752>, PMID: 8943330
- Trautmann S**, McCollum D. 2005. Distinct Nuclear and Cytoplasmic Functions of the *S. pombe* Cdc14-like Phosphatase Clp1p/Flp1p and a Role for Nuclear Shuttling in Its Regulation. *Current Biology* **15**:1384–1389. DOI: <https://doi.org/10.1016/j.cub.2005.06.039>
- Vavylonis D**, Wu JQ, Hao S, O’Shaughnessy B, Pollard TD. 2008. Assembly mechanism of the contractile ring for cytokinesis by fission yeast. *Science* **319**:97–100. DOI: <https://doi.org/10.1126/science.1151086>, PMID: 18079366
- Viana RA**, Pinar M, Soto T, Coll PM, Cansado J, Pérez P. 2013. Negative functional interaction between cell integrity MAPK pathway and Rho1 GTPase in fission yeast. *Genetics* **195**:421–432. DOI: <https://doi.org/10.1534/genetics.113.154807>, PMID: 23934882
- Wachowicz P**, Chasapi A, Krapp A, Cano Del Rosario E, Schmitter D, Sage D, Unser M, Xenarios I, Rougemont J, Simanis V. 2015. Analysis of *S. pombe* SIN protein association to the SPB reveals two genetically separable states of the SIN. *Journal of Cell Science* **128**:741–754. DOI: <https://doi.org/10.1242/jcs.160150>, PMID: 25501816
- Wagner E**, Glotzer M. 2016. Local RhoA activation induces cytokinetic furrows independent of spindle position and cell cycle stage. *Journal of Cell Biology* **213**:641–649. DOI: <https://doi.org/10.1083/jcb.201603025>, PMID: 27298323
- Willet AH**, McDonald NA, Gould KL. 2015. Regulation of contractile ring formation and septation in *Schizosaccharomyces pombe*. *Current Opinion in Microbiology* **28**:46–52. DOI: <https://doi.org/10.1016/j.mib.2015.08.001>, PMID: 26340438
- Willet AH**, DeWitt AK, Beckley JR, Clifford DM, Gould KL. 2019. NDR kinase Sid2 drives Anillin-like Mid1 from the membrane to promote cytokinesis and medial division site placement. *Curr Biol* **1063**:e1052. DOI: <https://doi.org/10.1016/j.cub.2019.01.075>
- Wu JQ**, Kuhn JR, Kovar DR, Pollard TD. 2003. Spatial and temporal pathway for assembly and constriction of the contractile ring in fission yeast cytokinesis. *Developmental Cell* **5**:723. DOI: [https://doi.org/10.1016/s1534-5807\(03\)00324-1](https://doi.org/10.1016/s1534-5807(03)00324-1), PMID: 14602073
- Wu JQ**, Sirotkin V, Kovar DR, Lord M, Beltzner CC, Kuhn JR, Pollard TD. 2006. Assembly of the cytokinetic contractile ring from a broad band of nodes in fission yeast. *The Journal of Cell Biology* **174**:391–402. DOI: <https://doi.org/10.1083/jcb.200602032>, PMID: 16864655
- Yeung T**, Gilbert GE, Shi J, Silviu J, Kapus A, Grinstein S. 2008. Membrane Phosphatidylserine Regulates Surface Charge and Protein Localization. *Science* **319**:210–213. DOI: <https://doi.org/10.1126/science.1152066>
- Yoshida S**, Kono K, Lowery DM, Bartolini S, Yaffe MB, Ohya Y, Pellman D. 2006. Polo-like kinase Cdc5 controls the local activation of Rho1 to promote cytokinesis. *Science* **313**:108–111. DOI: <https://doi.org/10.1126/science.1126747>, PMID: 16763112
- Zaitsevskaya-Carter T**, Cooper JA. 1997. Spm1, a stress-activated MAP kinase that regulates morphogenesis in *S. pombe*. *The EMBO Journal* **16**:1318–1331. DOI: <https://doi.org/10.1093/emboj/16.6.1318>, PMID: 9135147
- Zhou Z**, Munteanu EL, He J, Ursell T, Bathe M, Huang KC, Chang F. 2015. The contractile ring coordinates curvature-dependent septum assembly during fission yeast cytokinesis. *Molecular Biology of the Cell* **26**:78–90. DOI: <https://doi.org/10.1091/mbc.e14-10-1441>, PMID: 25355954